



Sudan University of Science and Technology

College of graduate studies

Department of Biomedical Engineering

***Development of Edge Detection Technique Using
Mathematics Methods for MRI Images***

تطوير تقنية كشف الحواف باستخدام طرق رياضية لصور جهاز الرنين المغناطيسي

Submitted in partial fulfillment of the requirement of M.Sc

Degree in Biomedical Engineering

By:

Hiba Almamoon Ali Jacknoon

Supervised By:

Dr. zeinab Adam Mustafa

March 2017

الآية

قال الله تعالى:

(قُلْ هَلْ يَسْتَوِي الَّذِينَ يَعْلَمُونَ وَالَّذِينَ لَا يَعْلَمُونَ إِنَّمَا يَتَذَكَّرُ أُولُو

الْأَلْبَابِ)

صدق الله العظيم

(الزمر: 9)

Acknowledgement

Foremost, I would like to express my sincere gratitude to my supervisor Dr. Zeinab Adam Mustafa for the continuous support of my MSc study and research, for her patience, motivation, enthusiasm, and immense knowledge. Her guidance helped me in all the time of research and writing of this thesis. I could not have imagined having a better supervisor and mentor for my MSc study.

Many of my friends have of great emotional and physical help; they have kept me stay sane through these difficult months. Their support and care helped me overcome setbacks and stay focused on my graduate study. I greatly value their friendship and I deeply appreciate their belief in me a deeply thanks to Mohammed Alsadiq, Ahmed Nageib, Husna, Esraa, Bayan, Shaza, Duaa, Marwa and all staff of radiologist and biomedical engineering in Zaitona Hospital. Most importantly, none of this would have been possible without the love and patience of my Parents and my Sister. This dissertation is dedicated to them, whom have been a constant source of love, concern, support and strength through these past months. Finally I also have to give a special mention for the effort and support given by Esraa Hashim and Emad Salah.

Abstract

Edge detection in medical image is an important task for object recognition of the human organs, and it is an essential pre-processing step in medical image segmentation and 3D reconstruction. Successful results of image analysis extremely depend on edge detection. Up to now many edge detection methods have been developed. But, they are sensitive to noise. This research discusses eight edge detection techniques in general, proposing Mathematics Edge Technique Filtering (METF) as a better technique. The mentioned technique goes through several steps, Starting with sharpening the image and separate it from the image, the filters will be applied to the resulting images. (wavelet filter and the bilateral filter) which were chosen based on a comparison with other filters applied MRI images after adding Gaussian noise to it, finally Graphical User Interface (GUI) was created with multiple options to edit images with different buttons offering variety of options, all what mentioned will be explained thoroughly on this thesis. Edge detection helps in optimizing network bandwidth and it is needed to keep track of data flowing in and out of the network. It helps to extract useful features for pattern recognition. Experiments results reveal that The METF technique is the best technique for our goals, were it had lower MSE and better SNR and PSNR.

المستخلص

الكشف عن الحواف في الصورة تؤدي دورا هاما في التعرف على الأعضاء البشرية وتمييزها، إذ يعد خطوة ما قبل المعالجة الأساسية في عملية تحليل الصور الطبية و تجزئتها واستخلاص معلومات معينة منها وإعادة بناء الصور ثلاثية الأبعاد. تم تطوير العديد من أساليب الكشف عن الحافة التي أثبتت كفاءتها في مجالات معينة وأعطت نتائج جيدة عند تطبيقها. ولكن تتمحور مشكلة هذه التقنيات في حساسيتها للضوضاء. وتناقش هذه الورقة ثمانية تقنيات لكشف الحافة بشكل عام، واقتراح تقنية الترشيح الرياضية للحافة للكشف عن الحواف (METF) كأفضل أسلوب. التقنية المذكورة مرت بعدة خطوات، بدءاً من زيادة حدة الصورة وفصل الحواف عن الصورة ثم استخدام مرشحات على الصور الناتجة (مرشح المويجات والمرشح الثنائي) اللذان تم اختيارهما اعتماداً على مقارنة بين عدة مرشحات طبقت على صورة جهاز الرنين المغناطيسي بعد إضافة ضوضاء جاونس لها. وأخيراً تم إنشاء واجهة المستخدم الرسومية (GUI) مع خيارات متعددة لتحرير الصور مع أزرار مختلفة تقدم مجموعة متنوعة من الخيارات، وجميع ما ذكر سيتم شرحها بشكل دقيق على هذه الرسالة. الكشف عن الحواف يساعد في تحسين عرض النطاق الترددي للشبكة، و تتبع تدفق البيانات داخل وخارج الشبكة. كما إنه يساعد على استخراج ميزات مفيدة للتعرف على الأنماط. نتائج التجارب تكشف أن تقنية الترشيح الرياضية للحافة للكشف عن الحواف هي أفضل تقنية لأهدافنا، حيث تمتلك أقل نسبة خطأ وأعلى معدل للإشارة بالنسبة للضوضاء مقارنة مع التقنيات الأخرى.

Table of Contents

Contents

الأية.....	I
Acknowledgement	II
Abstract.....	III
المستخلص.....	IV
Table of Contents.....	V
List of Figures.....	VIII
List of Tables	X
List of Abbreviations	XI
Chapter one	1
1 General Overview	1
1.1 Introduction.....	1
1.2 Objective	1
1.2.1 General.....	2
1.2.2 Specific	2
1.3 Problem statement.....	2
1.4 Layout	2
Chapter Two 2 Theoretical Background.....	3
2.1 MRI Scan	3
2.1.1 Uses of MRI.....	3
2.2 Image Definition	4
2.3 MRI scan image	6
2.4 Common Noises in MRI	7
2.5 Image Metrics	8
2.5.1 Mean Square Error (MSE)	8
2.5.2 Signal to Noise Ratio (SNR).....	8
2.5.3 Peak Signal to Noise Ratio (PSNR).....	9
2.6 Filtering.....	9
2.6.1 Lee Filter.....	10
2.6.2 Non-Local Means Filter.....	10
2.6.3 Bilateral Filter	11

2.6.4 Wavelet Thresholding filter	11
2.6.5 Anisotropic diffusion	12
2.6.6 Total variation denoising	13
2.6.7 Median filter.....	13
2.6.8 Speckle reduction anisotropic diffusion (SRAD) filter	13
2.6.9 Gaussian Filter	14
2.7 Edge Model Definition	15
2.8 Effects of noise on edge detection	16
2.9 Why Do We Need Edge Detection?	17
2.10 Difficulty with the Process of Edge Detection	17
2.11 Criteria for Edge Detection	18
2.12 Edge Detection Techniques	18
2.12.1 Robert's cross Operator	18
2.12.2 Prewitt's Operator	19
2.12.3 Laplacian of Gaussian (LoG).....	20
2.12.4 Canny's Edge Detection	20
2.12.5 Sobel Operator	21
Chapter Three.....	22
3 Literature Review.....	22
Chapter Four	25
4 Methodology	25
4.1 Noise addition and filtering	26
4.2 Edge detection technique	26
4.2.1 Wavelet transform.....	26
4.2.2 Unsharp mask.....	27
4.2.3 Structure, mathematics filtering (SMF)	27
4.2.4 Mathematics Edge TechniqueFiltering (METF).....	28
4.2.4.1 Using discrete wavelet transform (har).....	28
4.2.4.2 Using discrete Wavelet Thresholding filter	28
4.3 Graphical User Interface (GUI)	28
Chapter Five.....	30
5 Results and discussion	30
5.1 Results.....	30

5.1.1 Application of Spatial filters on noisy MRI image	30
5.1.2 Edge Detection Technique	34
5.1.3 Application of METF on Real MRI image	49
5.1.4 Graphical user interface (GUI)	51
5.2 Discussion	62
Chapter Six.....	63
6 Conclusion and Recommendation	63
6.1 Conclusion	63
6.2 Recommendation	63
References:.....	64

List of Figures

Figure 2-1: Image matrixes	4
Figure 2-2: Model of a digital image processing system.....	5
Figure 2-3: Gaussian distribution.....	15
Figure 2-4: Edges in image show object size, shape, boundary, human facial appearance.....	16
Figure 2-5: Roberts operator	19
Figure 2-7: Prewitt’s operator	20
Figure 2-8: (LoG) operator	20
Figure 2-9: Masks used by Sobel Operator.....	21
Figure 4-1 Block diagram of the proposed method	26
Figure 4-2: Discrete wavelet transform	27
Figure5-1: from a to j show the MRI scan image corrupted by Gaussian noise as a result of applying Spatial filters.....	32
Figure 5-2 : Plot of the performance of the Spatial Filters (given in table 5.1) according to the MSE (Blue), SNR (Orange), PSNR (Gray) for MRI image	33
Figure 5-3: Applying canny operator to original Image	34
Figure 5-4: Applying sobel operator to original Image	35
Figure 5-5: Applying prewitt operator to original Image	36
Figure 5-6: Applying operator LoG to original Image	37
Figure 5-7: Applying operator Roberts to original Image	38
Figure 5-8 : Applying discrete wavelet transformation technique (haar) to original Image.....	39
Figure 5-9: Applying Unsharp mask technique to original Image	40
Figure 5-10: Applying structure, mathematics filtering (SMF) technique to original Image.....	41
Figure 5-11: Applying Mathematics Edge Technique Filtering (METF) technique using discrete wavelet transform (har) and Bilateral filter to original Image.....	43
Figure 5-12: Applying Mathematics Edge Technique Filtering (METF) technique Using discrete Wavelet Thresholding filter and Bilateral filter to original Image	45
Figure 5-13: Histogram of original Image	46
Figure 5-14: Histogram of Applying Mathematics Edge Technique Filtering I (METF) technique to original Image	46

Figure 5-15: Histogram of Applying Mathematics Edge Technique Filtering II (METF) technique to original Image	47
Figure 5-16 : Plot of the performance of the edge detection technique according to the RMSE (Blue), SNR (Orange), and PSNR (Gray) for MRI image.....	48
Figure 5-17: show the abdominal at level of kidneys (bone window) MRI scan image after applying the METF edge detection techniques.	50
Figure 5-18 : Graphical User Interface (GUI)	51
Figure 5-19: use GUI to load image	52
Figure 5-21: From a to i Use GUI to show the results of applying the different types of filter to Gaussian noise image.	57
Figure 5-22: From a to i Use GUI to show the results of applying the edge detection techniques	61

List of Tables

Table 5-1: Statistical analysis of spatial filters for noisy MRI image (Gaussian noise)	32
Table 5-2: Statistical analysis of the edge detection technique for MRI.....	47

List of Abbreviations

- MRI** Magnetic resonance imaging
- NMR** nuclear magnetic resonance
- GUI** Graphical user interface
- RF** Radio frequency
- MRA** Magnetic Resonance Angiography
- RGB** red, green and blue
- MSE** Mean Square Error
- SNR** Signal to Noise Ratio
- PSNR** Peak Signal to Noise Ratio
- SRAD** Speckle redaction anisotropic diffusion
- NLM** Non local means
- SMF** Structure mathematics filtering
- METF** Mathematics Edge Technique Filtering
- MATLAB** Matrix Laboratory
- DWT** Discrete wavelet transformation

Chapter one

1 General Overview

1.1 Introduction

Medical imaging is the technique and process used to create images of the human body for clinical purposes or medical science^{[1][2][3]}. In image processing we can improve the image to appear it better i.e., in context of our information extraction from given image^[4]. Image processing is a type of signal processing in which image as an input and processes it by applying some operations on the selected pixels to get some useful information out of it. The early stages of vision processing identify features in images that are relevant to estimating the structure and properties of objects in a scene^[5].

Edges are one such feature. Edges are significant local changes in the image and are important features for analyzing images^[5]. Edges typically occur on the boundary between two different regions in an image. Edge detection is frequently the first step in recovering information from images. Due to its importance, edge detection continues to be an active research area^{[6][7]}.

Edge detection is one of the most commonly used operations in image analysis, and there are probably more algorithms in the literature for enhancing and detecting edges than any other single subject^[8]. Image Edge detection significantly reduces the amount of data and filters out useless information, while preserving the important structural properties^[9].

The function of edge detection is to identify the boundaries of homogeneous regions in an image based on properties such as intensity and texture. Many edge detection algorithms have been developed based on computation of the intensity gradient vector, which, in general, is sensitive to noise. Some image processing applications like segmentation need effective techniques that work as edge detection and extraction, many filters in this field fail to achieve the desired result and consequently the further processing fails, so it is needed sometimes to modify a technique to work in robust and effective way^[10].

1.2 Objective

The objectives of this research are general objective and specific objectives.

1.2.1 General

The major objectives of this project propose modify a technique for edge detection in medical MRI images.

1.2.2 Specific

- Enhancing MRI images
- Do comparisons study of MRI filters to reduce noise.
- Increase sharpness of the image.
- Development edge detection techniques.
- Graphical User Interface (GUI)

1.3 Problem statement

Many filters in this field fail to achieve the desired result in edge detection and consequently the further processing fails, so it is needed sometimes to modify a technique to work.

1.4 Layout

This project is structured as follows. Chapter one include introduction, objective, and problem statement; theoretical background were given in chapter two. Chapter three illustrates the literature review. Chapter four illustrates the research methodology; chapter five explores result of the thesis and discussion; chapter six includes; conclusion and recommendations.

Chapter Two

2 Theoretical Background

2.1 MRI Scan

Magnetic resonance imaging (MRI) is a medical imaging technique primarily used in radiology to generate anatomical and functional images of the human body. Also called Nuclear Magnetic Resonance (NMR). Unlike other medical imaging techniques, MRI does not use ionizing radiation and therefore is considered safer than many other techniques. Although not as sensitive as PET or SPECT, or as fast as CT, MRI is a very versatile technique able to generate great variety of image contrasts for a wide range of clinical and research applications. MRI detects signals predominantly from hydrogen nuclei (i.e., protons) in water or fat molecules. MRI signal acquisition is based on the phenomenon of nuclear magnetic resonance (NMR), which deals with the interactions between nuclear spins and magnetic fields^[11]. The main parts of the machine are: RF Coils, Gradient Coils, Magnet. Radio frequency (RF) fields are used to systematically alter the alignment of this magnetization, causing the hydrogen nuclei to produce a rotating magnetic field detectable by the scanner. This signal can be manipulated by additional magnetic fields to build up enough information to construct an image of the body. A radio frequency transmitter is briefly turned on, producing an electromagnetic field^[12].

2.1.1 Uses of MRI

MRI is used to image every part of the body, and is particularly useful for tissues with many hydrogen nuclei and little density contrast, such as the brain, muscle, connective tissue and most tumors. In clinical practice, MRI is used to distinguish pathologic tissue (such as a brain tumour) from normal tissue. Nonetheless the strong magnetic fields and radio pulses can affect metal implants and cardiac pacemakers. In the case of cardiac pacemakers, the results can sometimes be lethal, so patients with such implants are generally not eligible for MRI^[12].

The clinical applications of the MRI. T1 contrast is regularly used to generate anatomical images of various organs and tissues in the human body (e.g., white and gray matter in the brain), while T2 contrast is used to identify pathological tissues, like tumor or edema. Magnetic Resonance Angiography (MRA) is a technique that allows imaging of flowing blood in veins and arteries. In addition to imaging blood flow in the vessels, MRI is capable of measuring blood flow through capillaries in the tissue that is, tissue perfusion^[12].

2.2 Image Definition

An image is a spatial representation of a two-dimensional or three-dimensional scene. In image processing, an image usually is digitized from a recorded image, such as a video image, a camera or a picture. The digitization process includes sampling and quantization of continuous data. The sampling process samples the intensity of the continuous-tone image, such as a monochrome, color or multi-spectrum image, at specific locations on a discrete grid. The grid defines the sampling resolution. The quantization process converts the continuous or analog values of intensity brightness into discrete data, which corresponds to the digital brightness value of each sample, ranging from black, through the grays, to white. A digitized sample is referred to as a picture element, or pixel. An image is generally sampled into a rectangular array of pixels, which, for a monochrome image, is represented as a discrete matrix F :

$$F = \{f(x, y) \mid x=0, \dots, N-1, y=0, \dots, M-1\} \quad \text{Equation (2-1)}$$

Where N is total number of columns and M is total number of rows. The value of the image at spatial coordinates corresponding to the sample index (x, y) is denoted by $f(x, y)$, where x is the column number and y is the row number. The sample interval Δx and Δy are selected to match the smallest feature size. The physical coordinates are equal to $x \cdot \Delta$ and $y \cdot \Delta$. An example of an image matrix is shown in Figure 2.1.

Upper-left corner of image

	x							
		0	1	2	3	..		N-1
y	0	$f(0,0)$	$f(1,0)$	$f(2,0)$..		$f(N-1,0)$
1	$f(0,1)$	$f(1,1)$	$f(1,2)$..		$f(N-1,1)$
2	$f(0,2)$	$f(1,2)$	$f(2,2)$					
3								
4							:	
:							:	
M-1	$f(0,M-1)$	$f(1,M-1)$:	$f(N-1,M-1)$

Figure 0

For optical or photographic sensors, $f(x, y)$ is typically proportional to the radiant energy received in the electromagnetic band to which the sensor or detector is sensitive, and integrated over a small aperture around (x, y) . This is

interpreted as an intensity at point (x, y) . A simple aperture can be defined as a small rectangular or circular function in data acquisition processing, and the continuous intensity sampled is the integral of the image over the aperture at position (x,y) . Because of the integral effect, for example, the sharp edge in a real image will become a blurred edge in digital image. Normally digitized images are defined by levels of gray spanning from black to white, called gray scale images. Figure 2.2 shows the process of digital conversion.

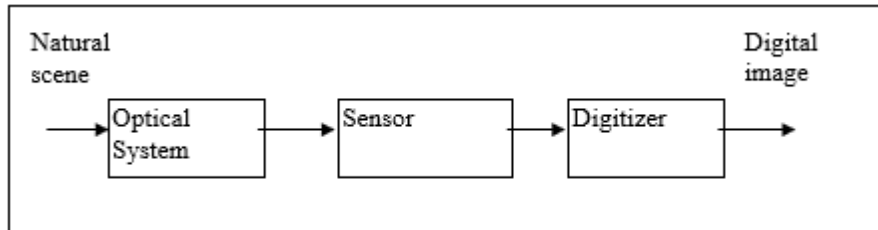


Figure 2-2: Model of a digital image processing system

Actually, the image information may come from different sources. For medical imaging applications the images can be digitized from x-rays, ultrasound waves, and Magnetic Resonance response. For astronomy and military applications, satellite sensors produce digital images directly from the measurements of reflected or emitted visible, infrared or microwave radiation. In auto vehicle navigation applications, a vision system may use a combination of passive and active spatial image data. During the image digitization, the image may be degraded by several factors. One is the restriction of sampling frequency. Based on the sampling theorem^[18], the image has to be sampled at a rate of at least twice the highest spatial frequency contained in original image. Otherwise the image will have spatial aliasing. In natural scenes there is no way to control the “highest spatial frequency”, and this theorem is almost never satisfied. The second factor is the blurring effect of aperture. The third one is the quantization error. Because the quantization uses a finite number of values to represent the infinite value range of original images, the intensity of an image is not exact. The fourth one is additive and multiplicative noise produced by quantization devices, such as thermal effects in electronic components, which is often modeled as Gaussian noise.

More naturally, if a color picture or multi-spectrum image is digitized in three channels: red, green and blue (RGB) respectively, the image can be represented in three intensity buffers. This is called a true color image because those three primary colors can generate wide ranges of colors perceived by the human visual system with the additive color mechanism. Although the RGB color space is one of the standard color spaces used to physically detect and generate colored light, other derivative color spaces can be created to aid color image processing. These alternate color spaces are

merely different methods of representing three components of color. The most important derivative color space is the hue, saturation and brightness (HSB) space^[19]. This color space represents color as we tend to perceive it. Instead of describing the red, green, and blue primary colors, HSB space describes the intuitive components of color. The hue component controls the color spectrum from red through the yellows, greens, blues, and violets. The saturation component controls the purity of the color, or how washed out the color is with white. The brightness component controls how bright the color appears.

In this thesis, we will restrict our discussion to the processing of gray scale images. Generally, all operations on gray scale images can be extended to process color images simply by applying them to each color component of the image, such as to intensity, or to hue, or to a single color component respectively.

2.3 MRI scan image

MRI uses the magnetic properties of spinning hydrogen atoms to produce images. The first step in MRI is the application of a strong, external magnetic field. For this purpose, the patient is placed within a large powerful magnet. Most current medical MRI machines have field strengths of 1.5 or 3.0 tesla (1.5T or 3T). The hydrogen atoms within the patient align in a direction either parallel or antiparallel to the strong external field. A greater proportion aligns in the parallel direction so that the net vector of their alignment, and therefore the net magnetic vector, will be in the direction of the external field. This is known as longitudinal magnetization. A second magnetic field is applied at right angles to the original external field. This second magnetic field is known as the radiofrequency pulse (RF pulse), because it is applied at a frequency in the same part of the electromagnetic spectrum as radio waves. A magnetic coil, known as the RF coil, applies the RF pulse. The RF pulse causes the net magnetization vector of the hydrogen atoms to turn towards the transverse plane, i.e. a plane at right angles to the direction of the original, strong external field. The component of the net magnetization vector in the transverse plane induces an electrical current in the RF coil. This current is known as the MR signal and is the basis for formation of an image. Computer analysis of the complex MR signal from the RF receiver coils is used to produce an MR image. Note that in viewing MRI images, white or light grey areas are referred to as 'high signal'; dark grey or black areas are referred to as 'low signal'. On certain sequences, flowing blood is seen as a black area referred to as a 'flow void'. Each medical MRI machine consists of a number of magnetic coils:

- 1.5T or 3T superconducting magnet.

- Gradient coils, contained in the bore of the superconducting magnet, used to produce variations to the magnetic field that allow image formation.
- Rapid switching of these gradients causes the loud noises associated with MRI scanning.
- RF coils are applied to, or around, the area of interest and are used to transmit the RF pulse and to receive the RF signal.
- RF coils come in varying shapes and sizes depending on the part of the body to be examined.
- Larger coils are required for imaging the chest and abdomen, whereas smaller extremity coils are used for small parts such as the wrist or ankle.^[17]

2.4 Common Noises in MRI

From theoretical expectations, the noise measured in unfiltered images was found to be normally distributed, spatially invariant and white . As in image processing, the digital images are much sensitive to noise which results are due to the image acquisition errors and transmission errors. MRI images captured usually are prone to speckle noise, Gaussian noise and salt and pepper noise which have influence on the image quality . Poor quality of image tends to degrade the performances of further works, e.g. feature extraction, reduction and classification of the processed images. The noises have to be removed before these processing stages as there were many available image filtering algorithms recommended in the literature.

Gaussian noise is a common noise distributed in magnitude MRI images and non-avoidable. Because of its mathematical tractability in both the spatial and frequency domains, Gaussian noise is used frequently in practice . Various filters such as average, median and adaptive Gaussian filter etc. have been proposed to clean the image from unfavourable candidates of noise. Salt and pepper noise also known as impulsive noise will have dark pixels and bright pixels alternate bright and dark regions. Because impulse corruption usually is large compared with the strength of the image signal, impulse noise generally is digitized as extreme values in an image . Speckle noise is a different type of noise in the coherent imaging of objects. Speckle noise is a granular noise which degrades the quality due to transmission errors^[14].

It is common practice to assume the noise in magnitude MRI images is described by a Gaussian distribution. The power of the noise is then often estimated from the standard deviation of the pixel signal intensity in an image region with no NMR signal. This can, however, lead to an approximately 60% underestimation of the true noise power. So the noise reduction in MR images is very important as a pre-processing task before going to image analysis and to improve the diagnostic quality of the images .

Thermal noise is the major source of noise in MR imaging. The MR images are reconstructed from the raw data by applying the inverse Fourier transform to it. The signal component is present in both real and imaginary channels which are orthogonal to each other and are affected by additive white Gaussian noise. Hence the noise in the reconstructed data is complex white Gaussian noise. Normally the magnitude image of the reconstructed complex data is used for visual inspection. So the magnitude of the MR signal is the square root of the sum of the squares of the data present in real and imaginary channels, the noise is the square root of the two independent Gaussian variables. Hence the noise in MR images is no longer Gaussian^[15].

Magnetic resonance (MR) images is usually modeled by means of a Rician distribution, due to the existence of zero-mean uncorrelated Gaussian noise with equal variance in both the real and imaginary parts of the complex k-space data . This noise may affect the performance of different postprocessing techniques applied to MR data, such as segmentation, registration or tensor estimation in diffusion tensor MRI (DT-MRI) . The image intensity of magnetic resonance images in the presence of noise is to be governed by a Rician distribution. Low signal intensities are therefore biased due to the noise. The noise can be estimated from the images and a simple scheme is describe to reduce the noise^[16].

2.5 Image Metrics

Image quality assessment is an emerging field of signal processing .More or less defined as the task of designing an algorithm to automatically judge the perceived “quality” of an image. Two of common measures are signal to noise ratio (SNR) and mean square error (MSE).

2.5.1 Mean Square Error (MSE)

Mean square error is a dominant quantitative performance metric in the field of image processing. It is used for the Assessment of image quality and fidelity. The cumulative squared error that occurs between compressed and original Form of image is termed as MSE. It is mathematically defined as:

$$MSE = \frac{1}{m*n} \sum_{i=1}^{n1} \sum_{j=1}^n (N(i,j) - DN(i,j))^2 \quad \text{Equation (2-2)}$$

Where m is the number of rows in the image, (i,j) is noisy image and $DN(i,j)$ is de-noised image^[20].

2.5.2 Signal to Noise Ratio (SNR)

Signal to noise ratio is a specification that measures the level of the audio signal compared to the level of noise present in the signal or by another meaning (signal to noise ratio is a comparison or ratio of the amount of signal

to the amount of noise and is expressed in decibels). Signal to noise ratio is abbreviated S/N Ratio and higher numbers mean a better specification. A component with a signal to noise ratio of 100dB means that the level of the audio signal is 100dB higher than the level of the noise and is a better specification than a component with a S/N ratio of 90dB. There are two methods of calculating the SNR. The first one defines the SNR as the ratio of the mean and the standard deviation of the measured signal.

$$SNR = \frac{\bar{x}}{\sigma} \quad \text{Equation (2-3)}$$

where \bar{x} = mean, σ = standard deviation.

The second method, which is mainly used in the field of electronics, the SNR is calculated as the ratio of the power of the signal P_{signal} to the power of the noise P_{noise} :

$$SNR = P_{signal} / P_{noise} = (v_{signal} / v_{noise})^2 \quad \text{Equation (2-4)}$$

Where the voltage V is the RMS voltage (root mean square voltage) [21]. The signal-to-noise ratio (SNR) is given by:

$$SNR = 10 \log_{10} \frac{\sum_{i=1}^M \sum_{j=1}^N (g_{i,j}^2 + f_{i,j}^2)}{\sum_{i=1}^M \sum_{j=1}^N (g_{i,j} - f_{i,j})^2} \quad \text{Equation (2-5)}$$

2.5.3 Peak Signal to Noise Ratio (PSNR)

PSNR is mathematically described as:

$$PSNR = 10 \log_{10} \left(\frac{R^2}{MSE} \right) \quad \text{Equation (2-6)}$$

Where R is the maximum fluctuation in the input image data type. For example, if the input image has a double precision data type, R=1. The PSNR value approaches infinity as the MSE approaches zero. Higher value of PSNR represents higher image quality. Small value of PSNR represents high numerical differences between images [20].

2.6 Filtering

The aim of any denoising method is to recover the original image from a noisy environment.

$$i = u(i) + n(i) \quad \text{Equation (2-7)}$$

Where i is the observed value, $u(i)$ is the actual or the true value and $n(i)$ is the noise perturbation at a pixel i . Several methods can be used to denoise and recover the true image u .

2.6.1 Lee Filter

The lee filter is a standard deviation based filter that calculates the new pixel value with statistics computed within individual filter windows. In lee filter, the statistical distribution of the values of the pixels within the moving kernel is utilized to estimate the value of the pixel of interest. This is based on the assumption that the mean and variance of the pixel of interest are equal to the local mean and local variance of all pixels within the user-selected moving kernel. The resulting grey level value R for the smoothed pixel is:

$$R = I_c * W + I_M * (1 - W) \quad \text{Equation (2-8)}$$

Where

$$W = \left(1 - \frac{c_u^2}{c_i^2}\right) \quad \text{Equation (2-9)}$$

$$C_u = \sqrt{1/\text{ENL}} \quad \text{Equation (2-10)}$$

$$C_i = \frac{s}{I_M} \quad \text{Equation (2-11)}$$

I_c = central pixel of filter window.

I_M = mean intensity within filter window.

S = standard deviation of intensity within filter window.

The weighting function W is a measure of the estimated noise variation coefficient C_u with respect to the image variation coefficient C_i . The number of looks parameter.

ENL is the effective number of looks of the radar image. ENL is used to estimate the noise variance and it controls the amount of smoothing applied to the image by the filter.

Moreover, ENL should be close to the actual number of looks, but it may be changed if the image has undergone resampling. The user may experimentally adjust the ENL value to control the effect of the filter. A small ENL value leads to more smoothing while a large ENL preserves more image features^[22].

2.6.2 Non-Local Means Filter

Is an algorithm in image processing for image de-noising. Unlike "local mean" filters, which take the mean value of a group of pixels surrounding a target pixel to smooth the image, non-local means filtering takes a mean of all pixels in the image, weighted by how similar these pixels are to the target pixel.

This results in much greater post-filtering clarity, and less loss of detail in the image compared with local mean algorithms^[23]. The NLM algorithm is defined by the formula:

$$NL[u](x) = \int_{\Omega} e^{-\frac{(Ga * |u(x+) - u(y+)|)^2}{h^2}} u(y) d\Omega \quad \text{Equation (2-12)}$$

$$u(x) = \frac{\int_{\Omega} e^{-\frac{(Ga * |u(x+) - u(y+)|)^2}{h^2}} u(y) d\Omega}{\int_{\Omega} e^{-\frac{(Ga * |u(x+) - u(y+)|)^2}{h^2}} d\Omega} \quad \text{Equation (2-13)}$$

Where $x \in \Omega$, Ωdz is normalizing constant, Ga is the Gaussian kernel and h acts as a filtering parameter.

According to this formula the de-noised value at x is the mean of all the values at all the points whose Gaussian neighborhood is as the neighborhood of x ^[20].

2.6.3 Bilateral Filter

The bilateral filter computes the filter output at a pixel as a weighted average of neighboring pixels. It smoothies the image while preserving edges. Due to this nice property, it has been widely used in noise reduction^[26], HDR compression^[35], multi-scale detail decomposition^[27], and image abstraction^[23]. It is generalized to the joint bilateral filter^[34], in which the weights are computed from another guidance image rather than the filter input. The joint bilateral filter is particular favored when the filter input is not reliable to provide edge information, e.g., when it is very noisy or is an intermediate result. The joint bilateral filter is applicable in flash/no-flash de-noising^[34], image up sampling^[28], and image de-convolution^[29]. However, it has been noticed^{[30][31][35]}, that the bilateral filter may have the gradient reversal artifacts in detail decomposition and HDR compression. The reason is that when a pixel (often on an edge) has few similar pixels around it, the Gaussian weighted average is unstable. Another issue concerning the bilateral filter is its efficiency. The brute-force implementation is in $O(Nr^2)$ time, which is prohibitively high when the kernel radius r is large^[32]. In an approximated solution is obtained in discretized space-color grid. Recently, $O(N)$ time algorithms have been developed based on histograms^{[33][24]}. Adam set al. ^[25] proposes a fast algorithm for color images. All the above methods require a high quantization degree to achieve satisfactory speed, but at the expense of quality degradation.

2.6.4 Wavelet Thresholding filter

Wavelet thresholding is one of the most popular approaches. In wavelet thresholding, a signal is decomposed into its approximation (low-frequency) and detail (high-frequency) sub-bands; since most of the image information is

concentrated in a few large coefficients, the detail s sub-bands are processed with hard or soft thresholding operations^[36].

Suppose we measure a noisy signal :

$$\mathcal{X}=s+v \quad \text{Equation (2-14)}$$

Assume s has a sparse representation in a certain wavelet bases, and $v \sim (0, \sigma^2 I)$

So

$$y=W^T \mathcal{X}=W^T s+W^T v=p+z \quad \text{Equation (2-15)}$$

Most elements in p are 0 or close to 0, and $E^Z \sim (0, \sigma^2 I)$

Since W is orthogonal, the estimation problem amounts to recovery of a signal in Gaussian noise. As p is sparse, one method is to apply a Gaussian mixture model for p.

Assume a prior $p \sim a(0, \sigma_1^2) + (1-a)\mathcal{N}(0, \sigma_2^2)$, σ_1^2 is the variance of "significant" coefficients, and σ_2^2 is the variance of "insignificant" coefficients.

Then

$$\tilde{p}=(p/y)=\tau(y)y \quad \text{Equation (2-16)}$$

Is called the shrinkage factor, which depends on the prior variances σ_1^2 and σ_2^2 . The effect of the shrinkage factor is that small coefficients are set early to 0, and large coefficients are unaltered. Small coefficients are mostly noises, and large coefficients contain actual signal^[37].

2.6.5 Anisotropic diffusion

Also called Perona–Malik diffusion, is a technique aiming at reducing image noise without removing significant parts of the image content, typically edges, lines or other details that are important for the interpretation of the image.

Anisotropic diffusion resembles the process that creates a scale space, where an image generates a parameterized family of successively more and more blurred images based on a diffusion process, this diffusion process is a linear and space-invariant transformation of the original image, Anisotropic diffusion is a generalization of this diffusion process. Anisotropic diffusion is a non-linear and space-variant transformation of the original image.

$(.,t):\Omega \rightarrow \mathbb{R}$ Be a family of gray scale images, then anisotropic diffusion is defined as

$$\frac{\partial I}{\partial t} = \text{div}(c(x,y,t)\nabla I) = \nabla c \cdot \nabla I + c(x,y,t)\Delta I \quad \text{Equation (2-17)}$$

Where Δ denotes the Laplacian, ∇ denotes the gradient, $di(\dots)$ is the divergence operator and $c(x,y,t)$ is the diffusion coefficient. (x,y,t) Controls the rate of diffusion and is usually chosen as a function of the image gradient so as to preserve edges in the image. Pietro Perona and Jitendra Malik pioneered the idea of anisotropic diffusion in 1990 and proposed two functions for the diffusion coefficient:

$$(\|\nabla I\|) = e^{-(\|\nabla I\|/K)^2} \quad \text{and} \quad c(\|\nabla I\|) = \frac{1}{1+(\|\nabla I\|/K)^2} \quad \text{Equation (2-18)}$$

The constant K controls the sensitivity to edges and is usually chosen experimentally or as a function of the noise in the image^[38].

2.6.6 Total variation denoising

Also known as total variation regularization is a process, most often used in digital image processing, that has applications in noise removal. It is based on the principle that signals with excessive and possibly spurious detail have high total variation, that is, the integral of the absolute gradient of the signal is high. According to this principle, reducing the total variation of the signal subject to it being a close match to the original signal, removes unwanted detail whilst preserving important details such as edges^[39]. We now consider 2D signals y , such as images. The total variation define as:

$$(y) = \sum_{i,j} \sqrt{|y_{i+1,j} - y_{i,j}|^2 + |y_{i,j+1} - y_{i,j}|^2} \quad \text{Equation (2-19)}$$

2.6.7 Median filter

The median filter is a nonlinear digital filtering technique, often used to remove noise. Such noise reduction is a typical pre-processing step to improve the results of later processing (for example, edge detection on an image). Median filtering is very widely used in digital image processing because, under certain conditions, it preserves edges while removing noise.

For 2D (or higher-dimensional) signals such as images, more complex window patterns are possible (such as "box" or "cross" patterns). Note that if the window has an odd number of entries, then the median is simple to define: it is just the middle value after all the entries in the window are sorted numerically. For an even number of entries, there is more than one possible median^[40].

2.6.8 Speckle reduction anisotropic diffusion (SRAD) filter

Casting the probability density function (PDE) approach and adaptive filtering approach Yongjian Yu et.al^[41] developed a new model for speckle reduction called as speckle reduction anisotropic diffusion (SRAD) method. SRAD filter can be seen as a mixture of the classical anisotropic diffusion filter and the adaptive speckle lee filter. The SRAD filter better preserves and

enhances edges while efficiently removing speckle in homogeneous regions. The SRAD anisotropic diffusion filter for smoothing a given image can be stated according to the following nonlinear partial differential equation.

For an intensity image $I_0(x,y)$ which is having finite power and no zero values over the image support Ω , the output image $I(x,y,t)$ is given by the following PDE.

$$\begin{cases} \partial I(x,y;t) / \partial t = \text{div}[c(q)\nabla(x,y;t)] \\ I(x,y;0) = I_0(x,y), (\partial I(x,y;t) / \partial n^{\rightarrow} |_{\partial\Omega} = 0 \end{cases} \quad \text{Equation (2-20)}$$

Where $\partial\Omega$ denotes the border of Ω , n^{\rightarrow} is the outer normal to $\partial\Omega$, and the diffusion coefficient (q) is expressed as

$$q = \frac{1}{1 + [q^2(x,y;t) - q_0^2(t)(1 + q_0^2(t))]} \quad \text{Equation (2-21)}$$

$$q = \exp \{ - [q^2(x,y;t) - q_0^2(t)] / [q_0^2(t)(1 + q_0^2(t))] \} \quad \text{Equation (2-22)}$$

With $q_0(t)$ standing for the speckle scale function. This coefficient is related to the local statistic of the image (mean and intensity variance over a homogeneous area at each t instant), but to do automatic image processing, it can be approximated by $q_0(t) \approx q_0 \exp[-pt]$, where p and q_0 are two positive parameter less than or equal to one. $(x,y;t)$ Is called the instantaneous coefficient of variation, and it is calculated from the image pixel intensity I , normalized gradient magnitudes $|\nabla I|/I$, and the normalized laplacian $\nabla^2 I/I$ as:

$$q(x,y;t) = \sqrt{\frac{(1/2)(|\nabla I|/I)^2 - (1/4^2)(\nabla^2 I/I)^2}{[1 + (1/4)(\nabla^2 I/I)]^2}} \quad \text{Equation (2-23)}$$

The above mentioned function, q which is the instantaneous coefficient of variation $(x,y;t)$ helps in detecting the edges present in the images corrupted by speckle. At edges and high contrast regions this function produces high values and at homogeneous regions it gives low values, $q_0(t)$ is the speckle scale function and $q(x,y;t)$ fluctuates around $q_0(t)$.

2.6.9 Gaussian Filter

Gaussian filtering is used to blur images and remove noise and detail. The Gaussian function is used in numerous research areas:

- It defines a probability distribution for noise or data.
- It is a smoothing operator.
- It is used in mathematics.

When working with images we need to use the two dimensional Gaussian function. This is simply the product of two 1D Gaussian functions (one for each direction) and is given by:

$$(X,Y) \frac{1}{2\pi\sigma^2} e^{-\frac{x^2+y^2}{2\sigma^2}} \quad \text{Equation (2-24)}$$

Where σ is the standard deviation of the distribution. A graphical representation of the 2D Gaussian distribution with mean $(0, 0)$ and $\sigma = 1$

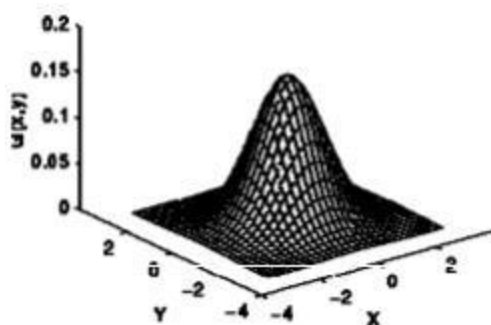


Figure 2-3: Gaussian distribution

The Gaussian filter is a non-uniform low pass filter. The kernel coefficients diminish with increasing distance from the kernel's Centre. Central pixels have a higher weighting than those on the periphery. Larger values of σ produce a wider peak (greater blurring). Kernel size must increase with increasing σ to maintain the Gaussian nature of the filter. Gaussian kernel coefficients depend on the value of σ . At the edge of the mask, coefficients must be close to 0. The kernel is rotationally symmetric with no directional bias. Gaussian kernel is separable which allows fast computation. Gaussian kernel is separable, which allows fast computation. Gaussian filters might not preserve image brightness.

2.7 Edge Model Definition

An edge corresponds to local intensity discontinuities of an image. In the real world, the discontinuities reflect a rapid intensity change, such as the boundary between different regions, shadow boundaries, and abrupt changes in surface orientation and material properties. For example, edges represent the outline of a shape, the difference between the colors and pattern or texture. Therefore, edges can be used for boundary estimation and segmentation in scene understanding. They can also be used to find corresponding points in multiple images of the same scene. For instance, the fingerprint, human facial appearance and the body shape of an object are defined by edges in images. In a broad sense the term edge detection refers to the detection and localization of intensity discontinuities of these image properties. In a more restrictive

sense, it only refers to locations of significant change of intensity. Points of these locations are called edges or edge elements. Figure 2.4 shows images in which edges define object size, shape, scene and human appearance.

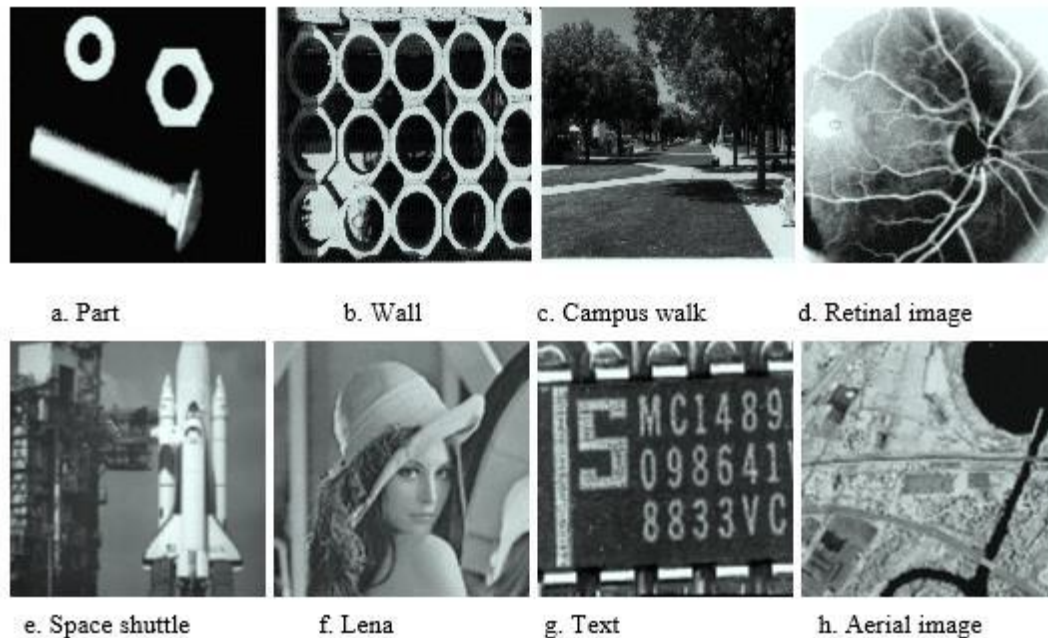


Figure 2-4: Edges in image show object size, shape, boundary, human facial appearance

The difference between boundaries and edges is that boundaries are the linked edges that characterize the shape of an object. Edges are piecewise segmentation. They are both useful in computation of geometrical features such as shape or orientation. Edge detection is grounded on the assumption that physical 3-dimensional shapes in the scene, such as object boundaries and shadow boundaries, are clues for the characterization of the scene.

2.8 Effects of noise on edge detection

Edge detection is susceptible to noise. This is due to the fact that the edge detectors algorithms are designed to respond to sharp changes, which can be caused by noisy pixels. Noise may occur in digital images for a number of reasons. The most commonly studied noises are white noise.

To reduce the effects of noise, preprocessing of the image is performed. The preprocessing can be performed in two ways, filtering the image with a Gaussian function, or by using a smoothing function. The problem with the above approaches is that the optimal result may not be obtained by using a fixed operator.

2.9 Why Do We Need Edge Detection?

In general, edge detection is the process that attempts to characterize the intensity changes in terms of the physical processes that have originated them. Edge detection can be used for region segmentation, feature extraction and object or boundary description. Edges provide the topology and structure information of objects in an image. For example, different cars can be easily recognized from their body shape. The highway and river from aerial images can be detected in terms of their structure or distribution pattern, which all are described by edges. By using edge detection techniques, machine vision and image processing systems can be built for a variety of applications. For example, edge detection can be used in assembly line inspection to detect defects of mechanical parts and in semiconductor manufactory. Edge detection can be used for locating the road and recognizing obstacles in automatic vehicle navigation. Edge detection also can be used to detect military targets in remote sensor applications. For medical imaging applications, edge detection and boundary segmentation can be used for locating tumors and blood vessels, and rigid bony structures.

Edge detection, therefore, is consistent with human visual response, which will provide edge strength and orientation for feature extraction and object description. For reducing information being processed, after edge detection gray scale edges are usually converted into binary images by thresholding. The transformation preserves a great deal of the primitive or intrinsic information from the original image, i.e., the outline of the shape. Later image processing can handle this simple form for recognition, matching or compression.

2.10 Difficulty with the Process of Edge Detection

Edge detection is a difficult issue. One difficulty comes from the complex contents of image itself. In real world applications, images contain object boundaries and object shadows and noise. The second cause of problems is degradation in image acquisition. Sometimes it may be difficult to distinguish the exact edge from noise or trivial geometric features. Two level edge detection processes are often used since the difficulty of edge estimation cannot be easily overcome from detection operators alone. The first level process, called low-level process, extracts pieces of raw edge segments and geometric features, called primitives. They may be incomplete and inaccurate. The second level process usually is called high-level process. It will interpret and combine raw edges based on the edge models or deduction rules from a broader image context and a knowledge database. Sometimes pattern matching and statistical analysis will occur at this level. The second level process tries to remove the uncertainty or make correct decisions using low-level inputs and context. The more accurate the low-level input is, the more accurate the high-level process result will be achieved. To measure the quality of low-level process, several criteria are proposed to help to improve the accuracy of edge detection.

2.11 Criteria for Edge Detection

The quality of edge detection can be measured from several criteria objectively. Some criteria are proposed in terms of mathematical measurement^[43], some of them are based on application and implementation requirements. In all cases a quantitative evaluation of performance requires use of images where the true edges are known.

Good detection: There should be a minimum number of false edges or maximum Signal Noise Ratio (SNR). Usually, edges are detected after a threshold operation. The high threshold will lead to less false edges, but it also reduces the number of true edges detected..

Noise sensitivity: The robust algorithm can detect edges in certain acceptable noise (Gaussian, Uniform and impulsive noise) environments. Actually, an edge detector

the edges and also amplifies the noise simultaneously. Strategic filtering, consistency checking and post processing (such as non-maximum suppression) can be used to reduce noise sensitivity^[42].

Good localization: The edge location must be reported as close as possible to the correct position, i.e. edge localization accuracy ^{[42][44]} .

Orientation sensitivity: The operator not only detects edge magnitude, but it also detects edge orientation correctly. Orientation can be used in post processing to connect edge segments, reject noise and suppress non-maximum edge magnitude.

Speed and efficiency: The algorithm should be fast enough to be usable in an image processing system. An algorithm that allows recursive implementation or parable processing can greatly improve efficiency.

Criteria of edge detection will help to evaluate the performance of edge detectors. Correspondingly, numerous techniques have been developed to achieve the targets listed above in terms of local region process, which can be classified into linear and nonlinear techniques.

2.12 Edge Detection Techniques

2.12.1 Robert's cross Operator

The Roberts Cross operator performs a simple, quick to compute, 2-D spatial gradient measurement on an image. Pixel values at each point in the output represent the estimated absolute magnitude of the spatial gradient of the input image at that point.

The operator consists of a pair of 2×2 convolution kernels as shown in Figure. One kernel is simply the other rotated by 90°. This is very similar to the Sobel operator.



Figure 2-5: Roberts operator

These kernels are designed to respond maximally to edges running at 45° to the pixel grid, one kernel for each of the two perpendicular orientations. The kernels can be applied separately to the input image, to produce separate measurements of the gradient component in each orientation (call these G_x and G_y). These can then be combined together to find the absolute magnitude of the gradient at each point and the orientation of that gradient. The gradient magnitude is given by:

$$|G| = \sqrt{G_x^2 + G_y^2} \quad \text{Equation (2-25)}$$

although typically, an approximate magnitude is computed using:

$$|G| = |G_x| + |G_y| \quad \text{Equation (2-26)}$$

which is much faster to compute^[45].

The angle of orientation of the edge giving rise to the spatial gradient (relative to the pixel grid orientation) is given by:

$$\theta = \arctan(G_y/G_x) - 3\pi/4 \quad \text{Equation (2-27)}$$

2.12.2 Prewitt's Operator

The Prewitt edge detection is proposed by Prewitt. To estimate the magnitude and orientation of an edge Prewitt is a correct way. Even though different gradient edge detection wants a quite time consuming calculation to estimate the direction from the magnitudes in the x and y-directions, the compass edge detection obtains the direction directly from the kernel with the highest response. It is limited to 8 possible directions; however knowledge shows that most direct direction estimates are not much more perfect. This gradient based edge detector is estimated in the 3x3 neighborhood for eight directions. All the eight convolution masks are calculated. One complication mask is then selected, namely with the purpose of the largest module.

-1	-1	-1
0	0	0
+1	+1	+1

G_x

-1	0	+1
-1	0	+1
-1	0	+1

G_y

Figure 2-7: Prewitt's operator

Prewitt detection is slightly simpler to implement computationally than the Sobel detection, but it tends to produce somewhat noisier results^[47].

2.12.3 Laplacian of Gaussian (LoG)

The Laplacian is a 2-D isotropic measure of the 2nd spatial derivative of an image. The Laplacian of an image highlights regions of rapid intensity change and is therefore often used for edge detection. The Laplacian is often applied to an image that has first been smoothed with something approximating a Gaussian Smoothing.

0	-1	0
-1	4	-1
0	-1	0

G_x

-1	-1	-1
-1	8	-1
-1	-1	-1

G_y

Figure 2-8: (LoG) operator

filter in order to reduce its sensitivity to noise. The operator normally takes a single gray level image as input and produces another gray level image as output^[45].

The Laplacian $L(x,y)$ of an image with pixel intensity values $I(x,y)$ is given by:

$$L(x,y) = \frac{\partial^2 I}{\partial x^2} + \frac{\partial^2 I}{\partial y^2} \quad \text{Equation (2-28)}$$

Since the input image is represented as a set of discrete pixels, we have to find a discrete convolution kernel that can approximate the second derivatives in the definition of the Laplacian^[45].

The Laplacian is generally used to found whether a pixel is on the dark or light side of an edge^[47].

2.12.4 Canny's Edge Detection

In industry, the Canny edge detection technique is one of the standard edge detection techniques. It was first created by John Canny for his Master's thesis at MIT in 1983, and still outperforms many of the newer algorithms that have

been developed. To find edges by separating noise from the image before find edges of image the Canny is a very important method. Canny method is a better method without disturbing the features of the edges in the image afterwards it applying the tendency to find the edges and the serious value for threshold^[47]. The algorithmic steps are as follows:

- Convolve image $f(r, c)$ with a Gaussian function to get smooth image $f^\wedge(r, c)$.
- $$f^\wedge(r, c) = f(r, c) * G(r, c, \sigma) \quad \text{Equation (2-29)}$$
- Apply first difference gradient operator to compute edge strength then edge magnitude and direction are obtain as before.
 - Apply non-maximal or critical suppression to the gradient magnitude.
 - Apply threshold to the non-maximal suppression image.

2.12.5 Sobel Operator

The operator consists of a pair of 3×3 convolution kernels as shown in Figure (2-9). One kernel is simply the other rotated by 90° .

-1	0	+1
-2	0	+2
-1	0	+1

G_x

+1	+2	+1
0	0	0
-1	-2	-1

G_y

Figure 2-9: Masks used by Sobel Operator

These kernels are designed to respond maximally to edges running vertically and horizontally relative to the pixel grid, one kernel for each of the two perpendicular orientations. The kernels can be applied separately to the input image, to produce separate measurements of the gradient component in each orientation (call these G_x and G_y). These can then be combined together to find the absolute magnitude of the gradient at each point and the orientation of that gradient^[47]. The gradient magnitude is given by:

$$|G| = \sqrt{G_x^2 + G_y^2} \quad \text{Equation (2-30)}$$

Typically, an approximate magnitude is computed using:

$$|G| = |G_x| + |G_y| \quad \text{Equation (2-31)}$$

which is much faster to compute^[46].

The angle of orientation of the edge (relative to the pixel grid) giving rise to the spatial gradient is given by:

$$\theta = \arctan(G_y/G_x) \quad \text{Equation (2-32)}$$

Chapter Three

3 Literature Review

In this chapter background material is provided, to make a brief description of the related work done by previous authors.

Milindkumar V. Sarode, Dr. Prashant R. Deshmukh, et al (2011), presented a Performance Evaluation of Noise Reduction Algorithm in Magnetic Resonance Images. The objective of this paper is to do the estimation of the noise in the Magnetic Resonance images and evaluate the noise reduction algorithm present in this paper. The method proposed specifically for Rician noise reduction, but because Rician noise can be approximated to Gaussian when SNR is high, therefore, they expect the proposed algorithm also has advantage in denoising of complex MR images.

V N Prudhvi Raj and Dr T Venkateswarlu, et al (2012), presented a Denoising of Magnetic Resonance and X-ray Images using Variance Stabilization and Patch based Algorithms, this paper presenting the Denoising techniques developed for removing the poison noise from X-ray images due to low photon count and Rician noise from the MRI, algorithm converting the Poisson and Rician noise distribution into Gaussian distribution, The results proved that the Anscombe transform, Freeman & Tukey transform with block matching 3D algorithm is giving a better result.

P.Deepa and M.Suganthi, et al (2014), presented a Performance Evaluation of Various Denoising Filters for Medical Image, This paper presents a review of some significant work in the area of image denoising filtering techniques applied to medical image. The performance of these techniques investigated the problem of image degradation which might occur during the acquisition of the images, optical effects such as out of focus blurring, camera motion, flat-bed scanner and video images.

Iza Sazanita Isa, Siti Noraini Sulaiman, Muzaimi Mustapha, Sailudin Darus, et al (2015), presented an Evaluating Denoising Performances of Fundamental Filters for T2-Weighted MRI Images In this work three different filtering algorithms Median filter (MF), Adaptive filter (ADF) and Average filter (AVF) are used to remove the additive noises present in the MRI images i.e. Gaussian, Salt and pepper and speckle noise. The performance of these filters are compared using the statistical parameters such as Mean Squared Error (MSE) and Peak Signal-to-Noise Ratio (PSNR). this study shows that the Median and Average filter produces better denoising results, preserving the main structures and details.

Canny, et al 1986.derived analytically optimal step edge operators and showed that the first derivative of Gaussian filter is a good approximation of such operators. An alternative to gradient techniques is based on statistical approaches.

Yahia S. Alhalabi, Hesham Jondi Abd, et al (2005), presented a New Wavelet-Based Techniques for Edge Detection, this paper applied the spatial domain methods, Thresholding and Edge based methods (Roberts operator, Sobel operator, Prewitt operator, and Laplacian operator). The resulting representation of wavelet transform provides an attractive tradeoff between spatial and frequency resolution where the human visual system can be better exploited. Also, wavelet transform reveals another important feature unfound in the conventional transforms in the sense that its basis function can be designed to exactly fit a given problem.

Raman Maini and J. S. Sobel, et al (2006) evaluated the performance of the Prewitt edge detector for noisy image and demonstrated that the Prewitt edge detector works quite well for digital image corrupted with Poisson noise whereas its performance decreases sharply for other kind of noise.

Tzu-Heng Henry Lee, et al (2008), presented an Edge Detection Analysis. This research paper presents a brief study of the fundamental concepts of the edge detection operation, theories behind different edge detectors, and some simple self-written Matlab edge detection functions with the simulation results. Previous works on edge detection models are reviewed and simulated. The Matlab results coincide with the first and second order derivative edge detection models.

Zhen Zhang, Siliang Maa, Hui Liu, Yuexin Gong, et al (2009), presented An edge detection approach based on directional wavelet transform, this paper propose an edge detection approach based on directional wavelet transform which retains the separable filtering and the simplicity of computations and filter design from the standard 2D WT. The experimental results of edge detection for several test images are provided to demonstrate approach.

M. Rama Bai, V. Venkata Krishna, J. SreeDevi.,et al (2010), presented a new Morphological Approach for Noise Removal cum Edge Detection in this paper proposes a novel approach for noise removal cum edge detection for both gray scale and binary images using morphological operations. Two images consisting of noise are processed and the effectiveness of the proposed approach is experimentally demonstrated.

J. Mehena., et al (2011), presented a Medical Images Edge Detection Based on Mathematical Morphology .In this paper, basic mathematical morphological theory and operations are introduced, and then a novel mathematical morphological edge detection algorithm is proposed to detect the edge of medical images with salt-and-pepper noise.

A. Singhal, M. Singh .,et al (2011), presented a Speckle Noise Removal and Edge Detection Using Mathematical Morphology. in This paper describes removal of speckle noise presented in images and then to obtain the useful edges in the output image obtained after noise removed using mathematical morphology.

Bindu Bansal, Jasbir Singh Saini, Vipin Bansal, and Gurjit Kaur, et al (2012), This paper compared several techniques for edge detection in image processing, Prewitts, Roberts, LoG and Canny.

A. Mehrotra, K. Kant Singh, M .J .Nigam., et al (2012), presented a Novel Algorithm for Impulse Noise Removal and Edge Detection. in This paper proposes a novel edge detection algorithm for images corrupted with noise. The algorithm finds the edges by eliminating the noise from the image so that the correct edges are determined.

S. Singh, N. Rup Prakash .,et al (2013), presented a Edge detection of Grey Scale Images based on Multi-Structure Elements Morphology. In This paper proposed a novel edge detection algorithm based on multi-structure elements morphology of eight different directions. Got five different edge detection results, then opening, closing, top hat transforms and bottom hat transform is used to get final results.

Jamila Harbi, Batool Daraam, Waseem M. Ali .,et al (2015), presented a Edge Detection in Ultrasound Images Basedon Modified Unsharp and Wavelet transform Filters. In this paper, two modified filters were suggested, first one is two-step unsharp filter. The second technique is summarized as adding back the Low-High and High-Low bands that were extracted previously from the original image by Haar wavelet transform to the image which reinforce its edges.

P. Mohankumar, Leong Wai Yie.,et al (2016), this study going to deal with the edge detection technique on scoliotic vertebrae and compare the performance of edge detectors using filters and operators.

Ahmed Nageib., et al, (2016), presented Development of edge detection technique using structure, mathematics filtering and graphical user interface (GUI) for CT images. In this thesis, a structure, mathematics filtering edge detection technique is proposed to detect medical image edge. A comparison was done between this technique and two other techniques (Discrete Wavelet Transform (haar), Unsharp mask). The results were judged by three metrics; mean square error (MSE), signal to noise ratio (SNR) and peak signal to noise ratio (PSNR).

Chapter Four

4 Methodology

The proposed method was developed using the MATLAB 2015 for the implementation of edge detection technique in medical image. This high performance language for technical computer, integrates computation, visualization, and programming in an easy-to-use environment. One of the reasons of selecting MATLAB in this thesis is because it fits perfectly in the requirements of an image processing research due to its inherent characteristics. Image Processing Toolbox of MATLAB provides a broad set of reference standard algorithms and graphical tools for image processing such as analysis, image enhancement, feature detection, noise reduction and image registration etc. Image processing toolbox supports a diverse set of image types, including high dynamic range, high resolution.

The images of MRI used in the implementation of the code were download from the siemens healthineers web. In this thesis a data set of MRI images were used. Then read and displayed the MRI images in the MATLAB software. These images processed prior to the application of the edge detection technique. The first step in processing the noise addition and several types of filters effective in removal of this type of noise applied to remove the noise. The next step comparing the values of the MSE, SNR and PSNR between the image corrupted by noise and the image after applying the filters. After This step done determined the best two filters to be used in the technique used to detect edges in this project. Then applied a number of well-known techniques to detect edges. It was edited and development in some of them to give the best results and then compared their results with the results of our technology is used to determine the effectiveness of our result in solving the problems, which have failed to resolve other techniques and then new technology applied and after comparing the result and clarity of its effectiveness have been applied to real pictures taken from real people from one of the hospitals in Khartoum state to test the effectiveness of this method is actually verify the validity solve the problems of magnetic resonance imaging. Finally it has been built graphical user interface (GUI) to view these results better.



Figure 4-1 Block diagram of the proposed method

4.1 Noise addition and filtering

In this step the Gaussian noise was added to the MR image. Several types of filters such as the anisotropic diffusion filter, Speckle Reducing Anisotropic Diffusion filter (SRAD), Mylee filter, Wavelet filter, Total variation filter, Gaussian filter, Median filter and Non local means filter were applied to the noisy image to remove the noise. The next step was comparing the values of the MSE, SNR, PSNR and Elapsed Time between the image corrupted by noise and the image after applying the filters. This step was done to determine the best two filters which are the wavelet and bilateral filters.

4.2 Edge detection technique

In this section nine techniques were applied, six of them operators: canny, sobel, prewite, laplacian of gaussian (LoG and roberts. It has been talk about them in detail in Chapter Tow. And other four masks rely on filters in its technology and its construction, Which: discrete wavelet transform (haar), unsharp mask and structure, mathematics filtering (SMF) and METF .

4.2.1 Wavelet transform

Haar is the simplest member of DWT (Discrete Wavelet Transform) family, its procedure is to scan the square image in two steps horizontally and vertically indicating Low-Low, Low-High, High-Low and High-High frequencies in four portions in the resultant image. In this part the Low-High (LH) and High-Low (HL) portion of Haar wavelet transform were used because these two bands consist of the most edge details of the image scanned horizontally and vertically, Low-Low (LL) has no useful edges due to the most details of the image included and conversely the High-High (HH) has very rare high intensity pixels which generally form no explicit edges, then adding these two bands (LH and HL) to the original image reinforces its edges. The two bands (LH and HL) were added to the image obtained from the previous step as shown in figure 5-13 in the result.

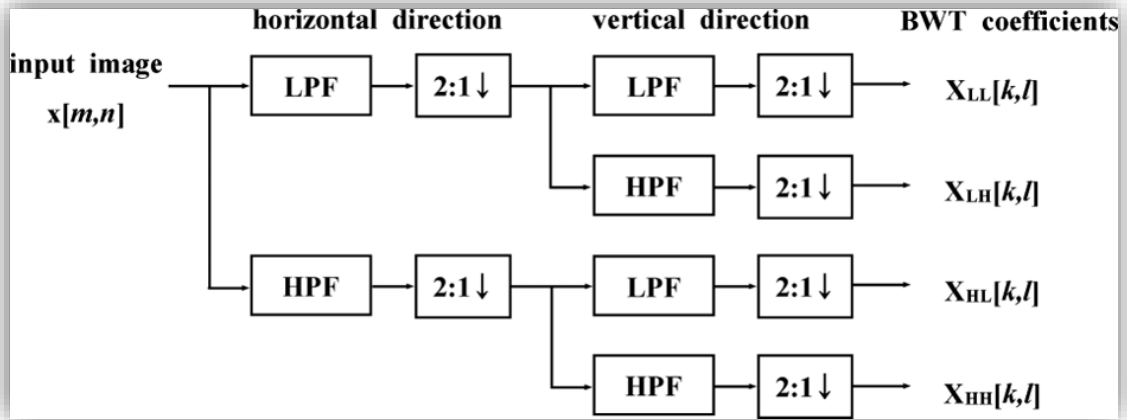


Figure 4-2: Discrete wavelet transform

4.2.2 Unsharp mask

In this part a Gaussian filter with mask (5*5) was applied to blur the original image. The blurred image (I_{blur}) was subtracted from the original image ($I_{original}$) and the result of this process is an image with edges (I_{edge}).

$$I_{edge}(i,j) = I_{original}(i,j) - I_{blur}(i,j) \quad \text{Equation (4-1)}$$

The enhanced image ($I_{enhanced}$) is a result of adding the original image to the image with edges multiplied by a scaling factor k which is an arbitrary value varies between 0.2 to 0.7; preventing the excess of each pixel value over 255 in common uint8 grayscale images. In this step the value of $k=0.5$.

$$I_{enhanced}(i,j) = I_{original}(i,j) + k * I_{edge}(i,j) \quad \text{Equation (4-2)}$$

Finally the modified image is the result of adding the original image to the enhanced image multiplied by a scaling factor $k=0.3$.

$$I_{modified}(i,j) = I_{enhanced}(i,j) + k * I_{edge}(i,j) \quad \text{Equation (4-3)}$$

4.2.3 Structure, mathematics filtering (SMF)

In this part a sharpen filter was applied to the image, then the sharpened image was subtracted from the original image to obtain an image with edges. The next step was applying the Non Local Means to the sharpen image, and Lee filter was applied to the image obtained from subtracting the original image from the sharpened image, then the two images obtained from the previous steps were added together and the resultant image was multiplied by a scaling factor k .

4.2.4 Mathematics Edge Technique Filtering (METF)

4.2.4.1 Using discrete wavelet transform (har)

In this technique applied sharpen filter to the original image, then subtracted the sharpened image from the original image.

$$I_{edge} = I_{original} - I_{sharp} \quad \text{Equation (4-4)}$$

this subtracted resulted an edge, this edge added to original image.

$$I_{edge*} = I_{edge} + I_{original} \quad \text{Equation (4-5)}$$

after that applied the discrete wavelet transform (har) to the sharpened image (added these two bands (LH and HL) to the sharpened image).

$$I_{Har} = I_{HL} + I_{LH} + I_{sharp} \quad \text{Equation (4-6)}$$

Then bilateral filter was applied to the image obtained from subtracting the original image from the sharpened image. Finally the images obtained from added edge to original image, image after applied the discrete wavelet transform and the image obtained from applied bilateral filter were added together

$$I_{result} = I_{Har} + I_{bilateral} + I_{edge*} \quad \text{Equation (4-7)}$$

All techniques and filters used in this project were converted to functions to simplify the use of the Graphical User Interface (GUI) in the next section.

4.2.4.2 Using discrete Wavelet Thresholding filter

Is the similar Technique to the previous Technique (Using discrete wavelet transform), but deferent in applied the Wavelet Thresholding filter to the sharpened image.

All techniques and filters used in this project were converted to functions to simplify the use of the Graphical User Interface (GUI) in the next section.

4.3 Graphical User Interface (GUI)

In this section the GUI was created using the command “guide” in the Matlab command window. This will open a window with two options create new GUI or open existing GUI. To create a new GUI select “create new GUI” option. This option opens a window with other options such as blank GUI (default) and GUI with Uicontrols etc., the option chosen here is “Blank GUI”, this option opens another window this window contains the parameters used in the interface.

The interface consists of four axes one for the original image and noise image, two for images after applied denoising filters, three for images resulted from applied edge detection techniques and four for image resulted after METF. Three button groups (a group for loading original and noising images, group for filtering (anisotropic diffusion filter, Gaussian filter, Bilateral filter, Total variation filter, SRAD filter, Lee filter, Wavelet filter, Median filter and Non local means filter) and group for edge detection techniques(Canny, Sobel, Prewitt, Laplacian of Gaussian(LoG), , Roberts, wavelet (haar), Unsharp mask and SMF), The Three button groups consist of twenty push buttons which are:

Load: for loading original image (manipulated) to the GUI.

Noise: add Gaussian noise.

Lee: filter to remove noise from image.

Median: filter to remove noise from image.

Anisotropic diffusion filter: filter to remove noise from image.

Wavelet: filter to remove noise from image.

NLM: filter to remove noise from image.

Gaussian: filter to remove noise from image.

Bilateral: filter to remove noise from image.

SRAD: filter to remove noise from image.

Total variation: filter to remove noise from image.

Canny: edge detection technique.

Sobel : edge detection technique.

Prewitt: edge detection technique.

Laplacian of Gaussian(LoG): edge detection technique.

Roberts: edge detection technique.

Wavelet (Haar): edge detection technique.

Unsharp mask: edge detection technique.

SMF: edge detection technique.

MFE: edge detection technique.

Chapter Five

5 Results and discussion

5.1 Results

The result is divided into four parts; application of Spatial filters on noisy MRI image, edge detection technique, application METF on real image and graphical user interface (GUI).

5.1.1 Application of Spatial filters on noisy MRI image

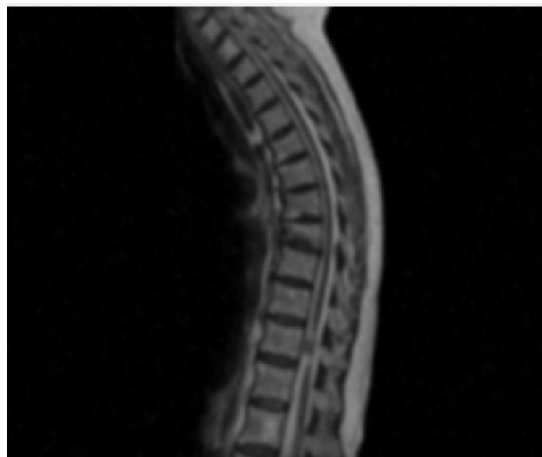
Noisy MRI image was filtered with the following spatial filters: anisotropic diffusion filter, Speckle Reducing Anisotropic Diffusion filter (Srad), Lee filter, Bilateral filter, Wavelet filter, Total variation filter, Gaussian filter, Median filter and Non local means filter, the images below show the result after applying the Spatial filters to the image:



a) Original Image



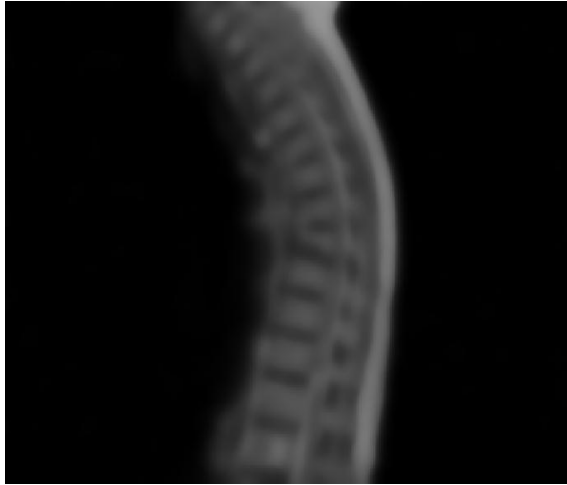
b) Image corrupted by Gaussian noise



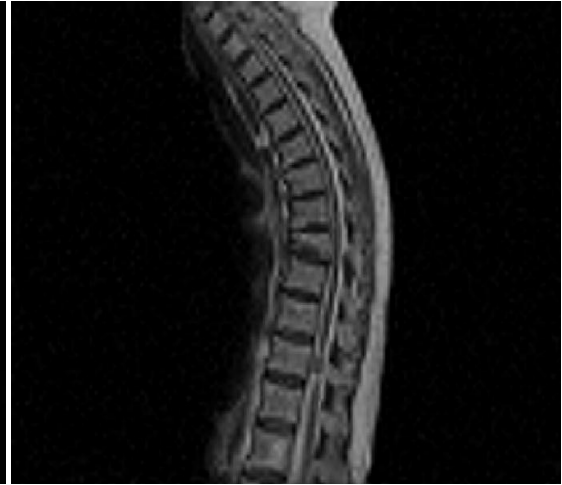
c) Image after applying Gaussian filter



d) Image after applying SRAD filter



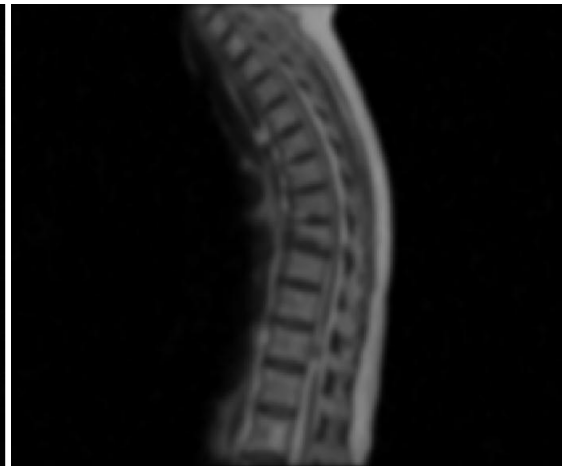
e) Image after applying total variation filter



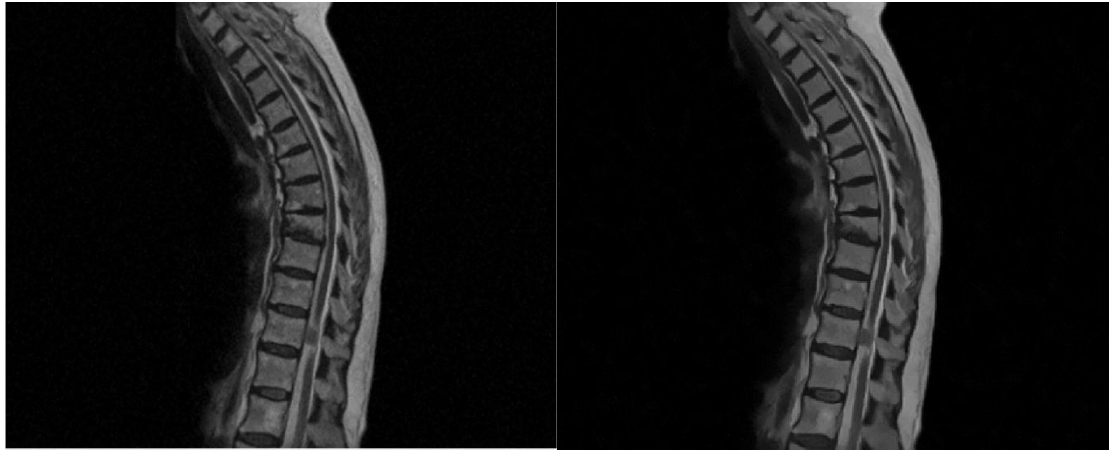
f) Image after applying wavelet filter



g) Image after applying Bilateral filter



h) Image after applying anisotropic filter



i) Image after applying Median filter

j) Image after applying Non Local Means filter

Figure5-1: from a to j show the MRI scan image corrupted by Gaussian noise as a result of applying Spatial filters.

Figure(5-1) from a to j show the MRI scan image corrupted by Gaussian noise as a result of applying Spatial filters: (Gaussian filter, Speckle Reducing Anisotropic Diffusion filter (Srad), Total variation filter, Wavelet filter, Bilateral filter, anisotropic diffusion filter, Median filter, and the Non local means filter.

Table 5-1: Statistical analysis of spatial filters for noisy MRI image (Gaussian noise)

Filter name	MSE	SNR	PSNR	Elapsed Time(seconds)
Non local means	0.0425	11.8978	27.4098	156.017031
Srad	0.2256	2.3178	13.1841	0.56072
Total variation	0.0685	7.6975	23.2085	0.527259
Wavelet	0.0538	9.8956	25.3979	0.298645
Gaussian	0.0558	9.5628	25.0672	0.796556
Bilateral	0.052	50.3788	65.8908	3.929778
anisotropic diffusion	0.0632	8.4762	23.9731	0.378655
Median	0.0385	12.7859	28.2857	37.400303

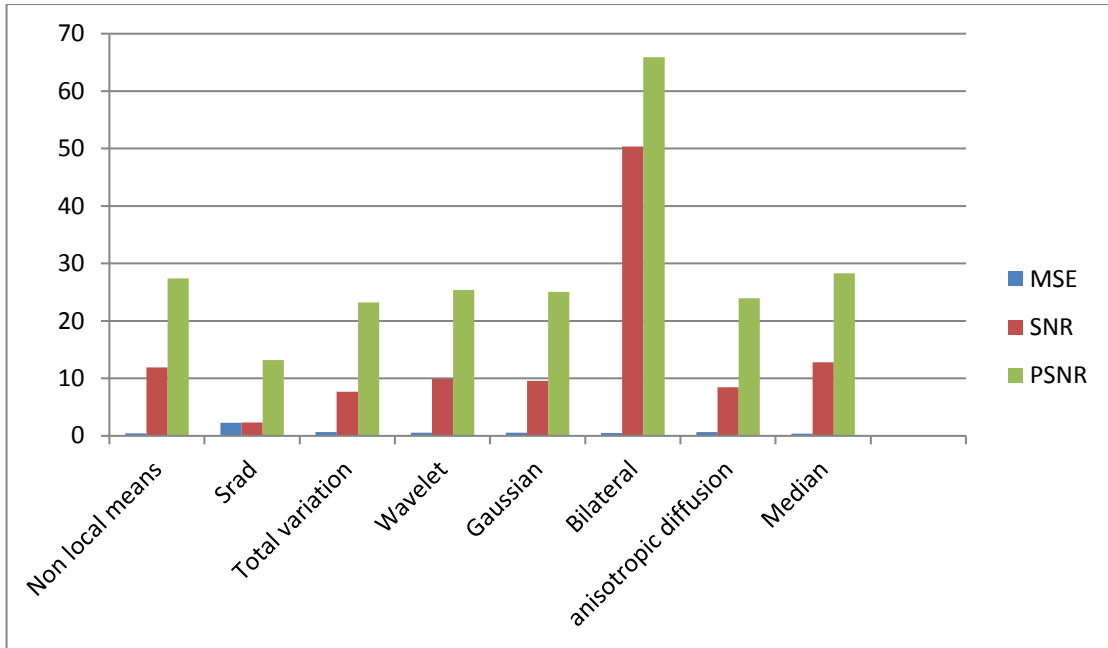


Figure 5-2 : Plot of the performance of the Spatial Filters (given in table 5.1) according to the MSE (Blue), SNR (Orange), PSNR (Gray) for MRI image

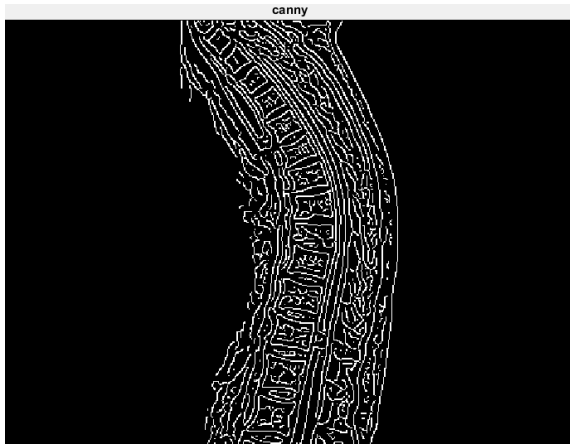
5.1.2 Edge Detection Technique

In this section, the edge detection techniques were applied and the results are shown as follows:

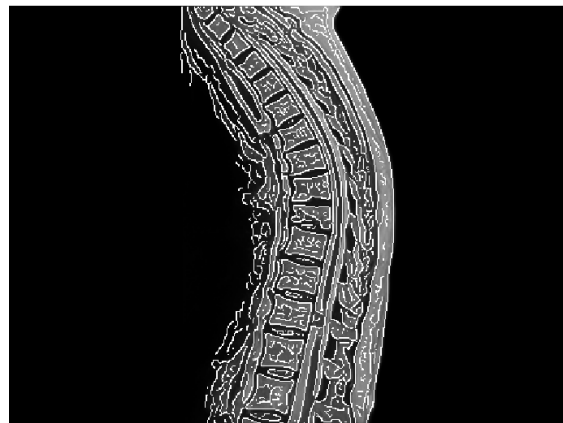
Canny Operator



a)Original image



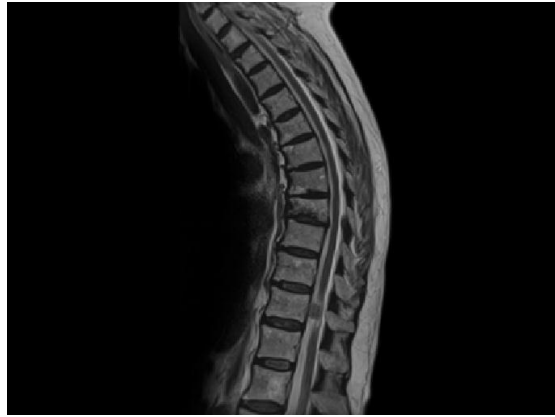
b)Result of canny operator



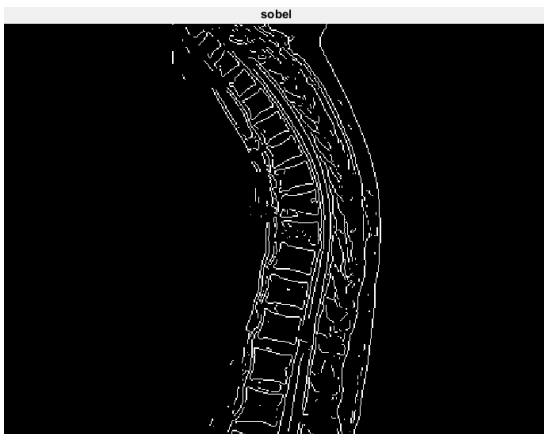
c) Addition canny operator to original image

Figure 5-3: Applying canny operator to original Image

Sobel Operator



a)Original image



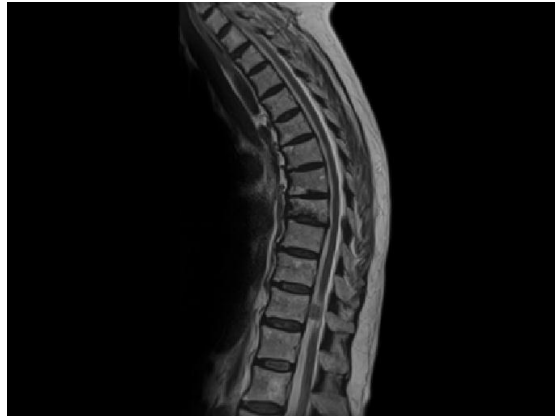
b)Result of sobel operator



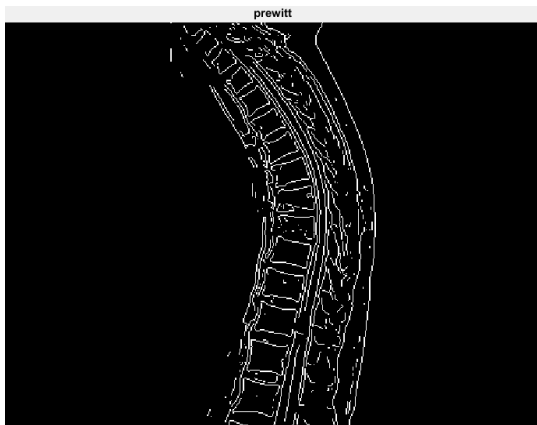
c) Addition sobel operator to original image

Figure 5-4: Applying sobel operator to original Image

Prewitt Operator



a)Original image



b)Result of prewitt operator



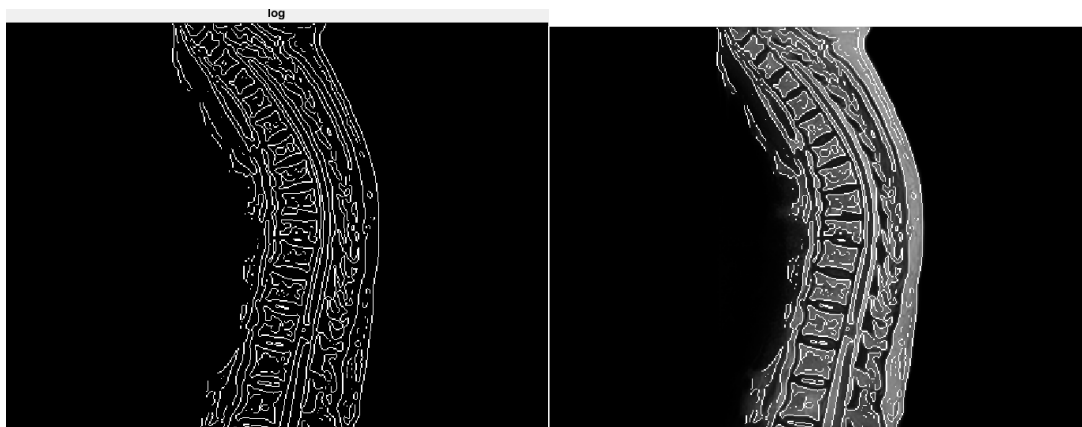
c) Addition prewitt operator to original image

Figure 5-5: Applying prewitt operator to original Image

Laplacian of Gaussian(LoG) Operator



a)Original image



b)Result of LoG operator

c) Addition LoG operator to original image

Figure 5-6: Applying operator LoG to original Image

Roberts Operator



a)Original image



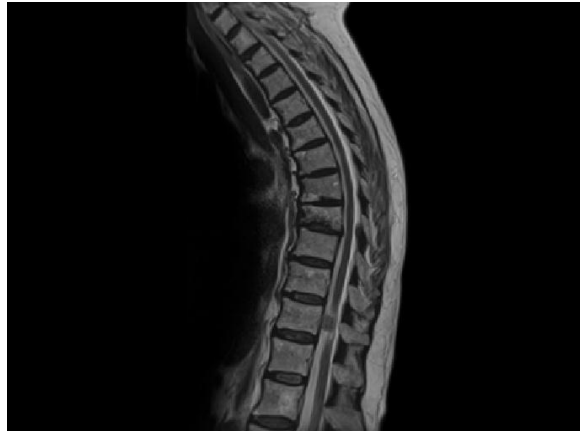
b)Result of Roberts operator



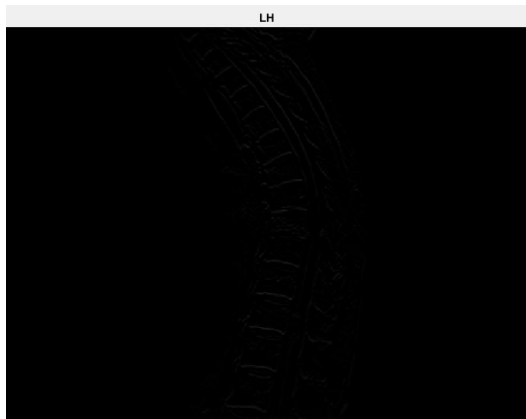
c) Addition Roberts operator to original image

Figure 5-7: Applying operator Roberts to original Image

Discrete wavelet transformation (haar)



a) Original image



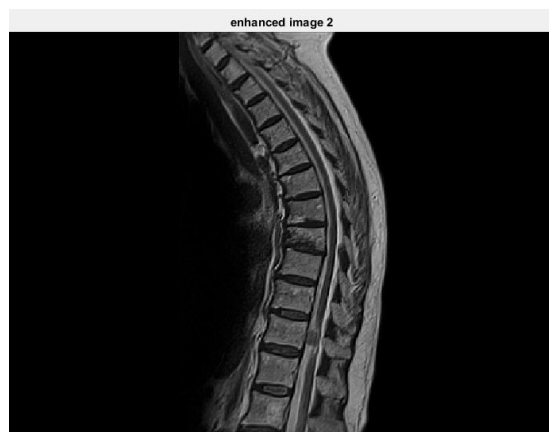
b) LH of wavelet transformation



c) HL of wavelet transformation



d) Result of wavelet technique



e) Result of enhance wavelet technique

Figure 5-8 : Applying discrete wavelet transformation technique (haar) to original Image

Unsharp mask



a)Original image



b) blurred image by Gaussian filter



c) subtraction blurred image from the original image



d) addition of subtracted image to the original image



e) Result of enhance Unsharp mask

Figure 5-9: Applying Unsharp mask technique to original Image

Structure, mathematics filtering (SMF)



a) original image



b) applying sharpen to the original image



c) subtraction of sharpen from the original image



d) addition of subtracted and sharpen images to the original image

Figure 5-10: Applying structure, mathematics filtering (SMF) technique to original Image

Mathematics Edge Technique Filtering (METF)

I) Using discrete wavelet transform (har) and Bilateral filter



a) original image



b) applying sharpen to the original image



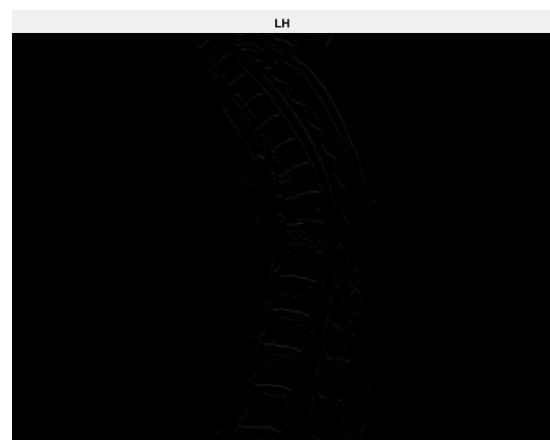
c) subtraction of sharpen from original image



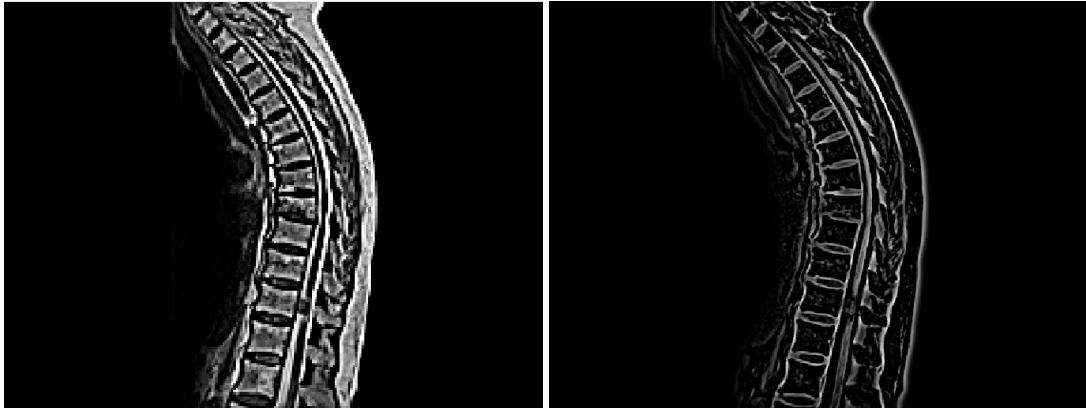
d) addition of subtracted to the original image



e) HL of wavelet transformation



f) LH of wavelet transformation



g) Result of addition of HL and LH of wavelet transformation to sharpen image

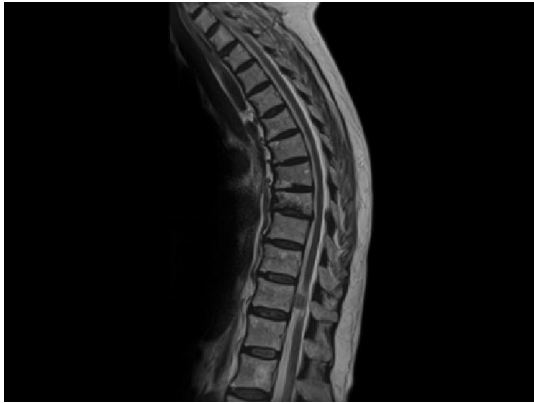
h) Result of filtering subtraction of sharpen from original image by bilateral filter



i) Result of addition of wavelet transformation and filtering subtracted and subtracted to original image

Figure 5-11: Applying Mathematics Edge Technique Filtering (METF) technique using discrete wavelet transform (har) and Bilateral filter to original Image

II) Using discrete Wavelet Thresholding filter



a) original image



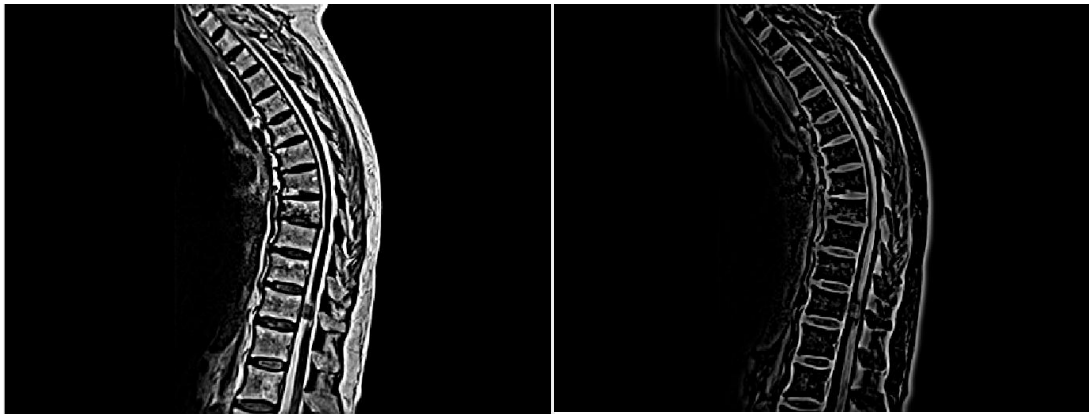
b) applying sharpen to the original image



c) subtraction of sharpen from original image



d) addition of subtracted to the original image



e) Result of filtering sharpen image by Wavelet Thresholding filter

f) Result of filtering subtraction of sharpen from original image by bilateral filter



g) Result of addition of wavelet transformation and filtering subtracted and subtracted to original image

Figure 5-12: Applying Mathematics Edge Technique Filtering (METF) technique Using discrete Wavelet Thresholding filter and Bilateral filter to original Image

Figures from 5-3 to 5-12 show the Total Spine (T-Spine) MRI scan image after applying the edge detection techniques using canny Operator, sobel operator, prewitt operator, (LoG) operator, roberts operator, the discrete wavelet transform, unsharp mask, the structural mathematics filtering technique (SMF) and mathematics edge technique filtering (METF).

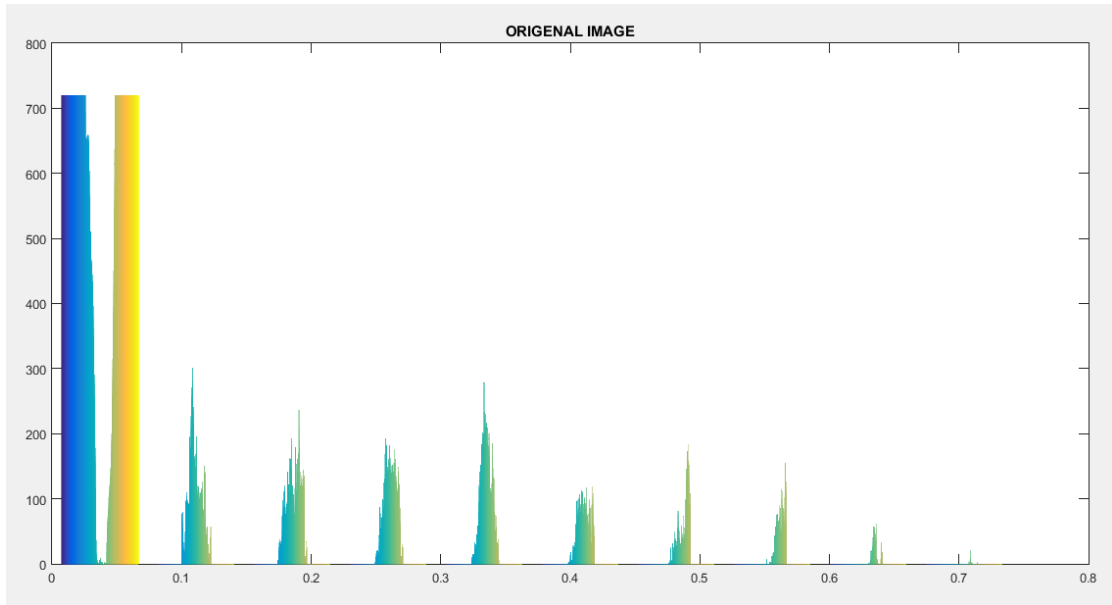


Figure 5-13: Histogram of original Image

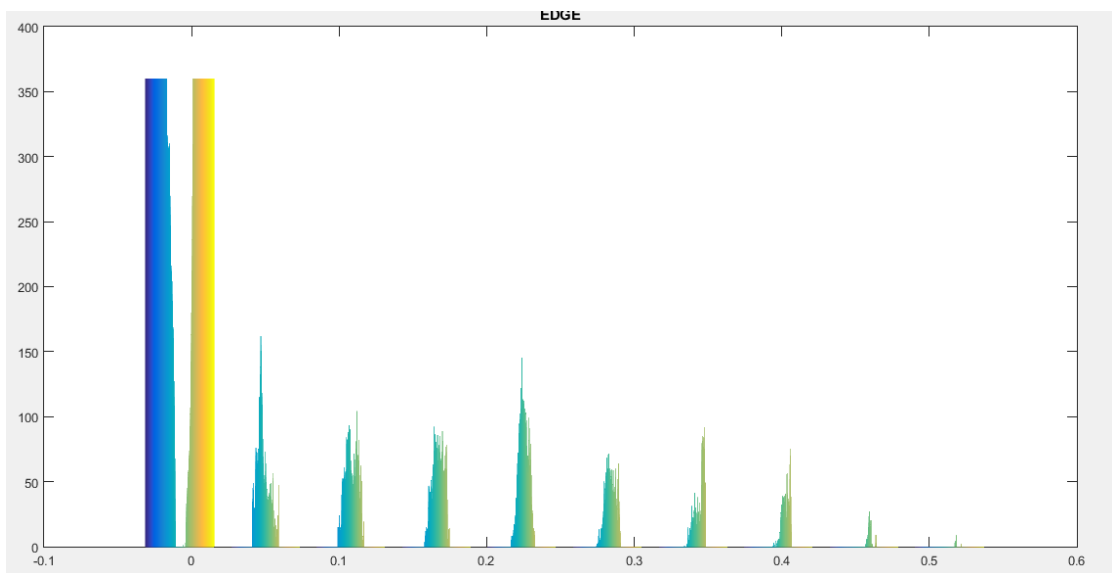


Figure 5-14: Histogram of Applying Mathematics Edge Technique Filtering I (METF) technique to original Image

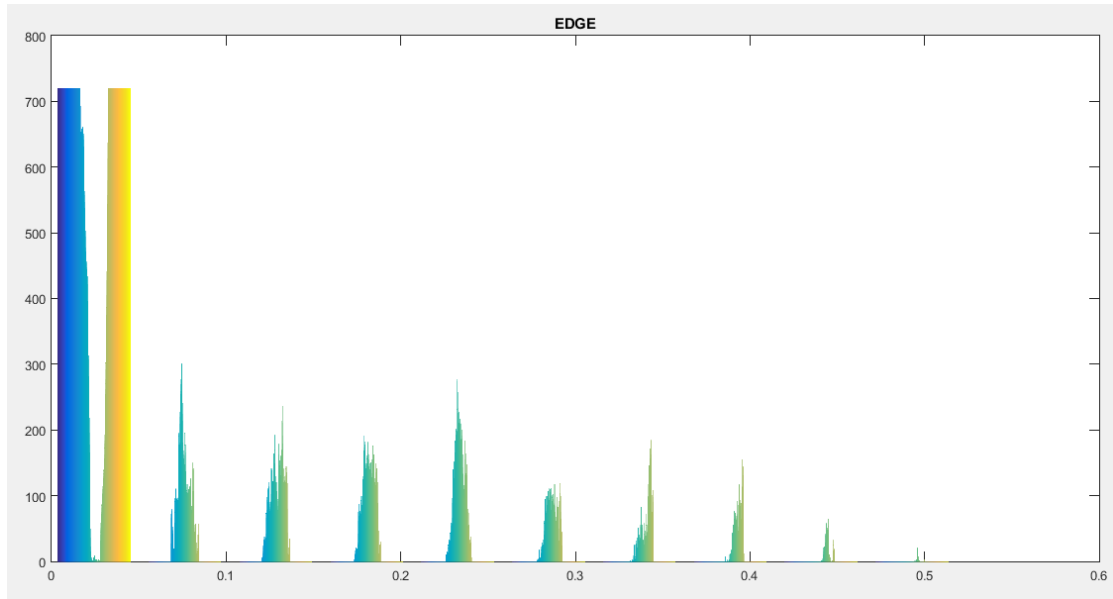


Figure 5-15: Histogram of Applying Mathematics Edge Technique Filtering II (METF) technique to original Image

Table 5-2: Statistical analysis of the edge detection technique for MRI

Edge detection	MSE	SNR	PSNR	Elapsed Time(seconds)
Canny	0.2467	3.7545	12.1569	0.439002
Sobel	0.1744	0.7401	15.1714	0.330409
Prewitt	0.1731	0.6759	15.2355	0.354913
Laplacian of Gaussian(LoG)	0.2097	2.343	13.5684	0.388092
Roberts	0.184	1.2083	14.7031	0.427426
UNSHARP	0.2184	16.8093	32.7133	1.037835
HAR OR WAVELET	0.0364	18.8832	34.7946	1.428123
SMF	0.0558	10.2012	26.1053	595.848978
METF I	0.0182	18.8832	34.7944	14.1569
METF II	0.0478	54.3243	70.2284	14.445305

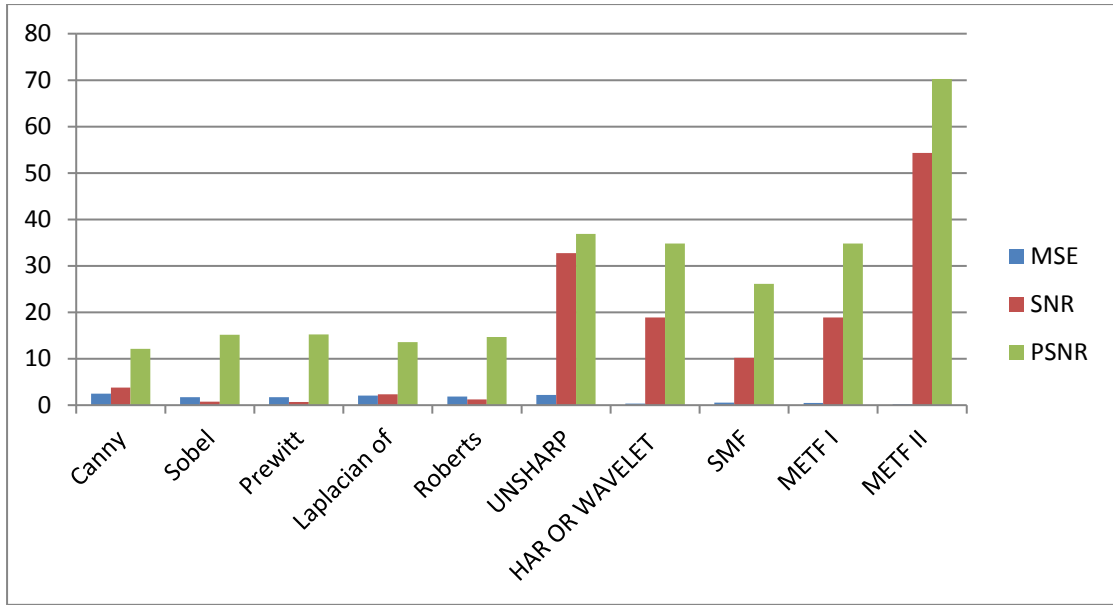
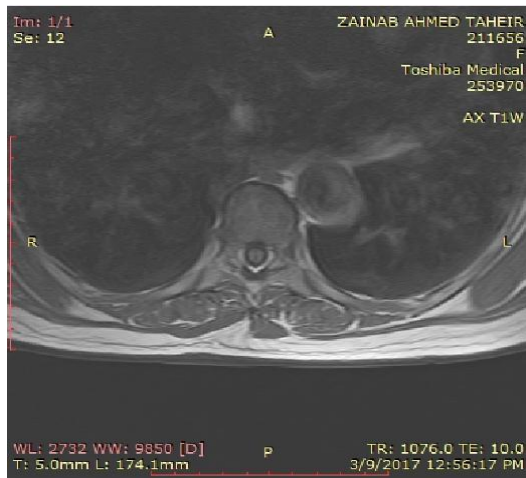


Figure 5-16 : Plot of the performance of the edge detection technique according to the RMSE (Blue), SNR (Orange), and PSNR (Gray) for MRI image.

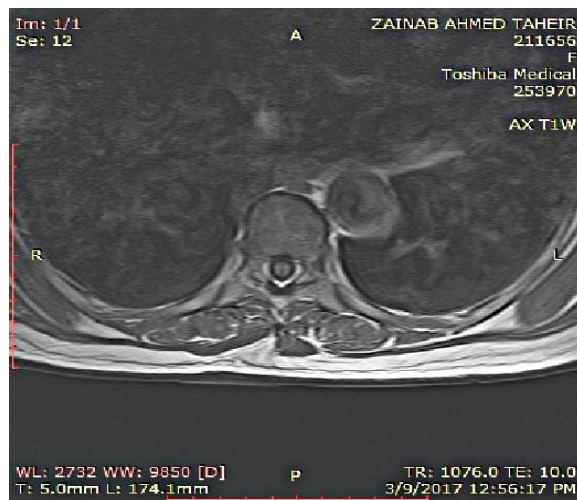
5.1.3 Application of METF on Real MRI image



a) original image (1)



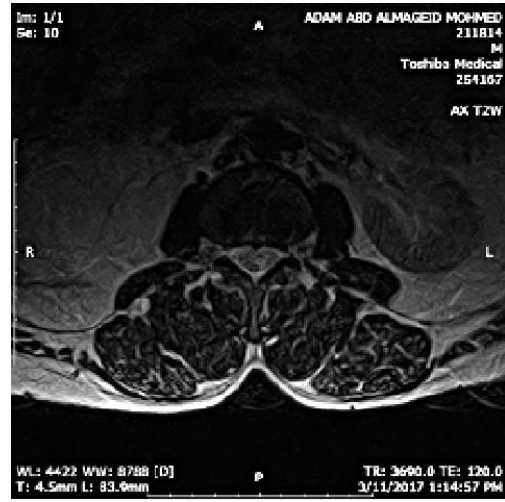
b) applying METF I to original image



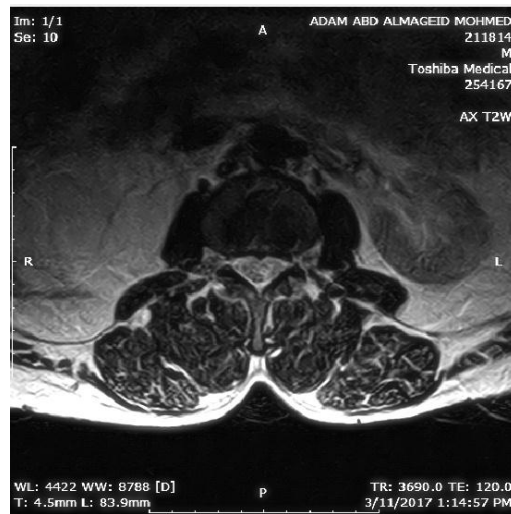
c) applying METF II to original image



d) original image (2)



e) applying METF I to original image



f) applying METF II to original image

Figure 5-17: show the abdominal at level of kidneys (bone window) MRI scan image after applying the METF edge detection techniques.

5.1.4 Graphical user interface (GUI)

In this section the GUI was applied

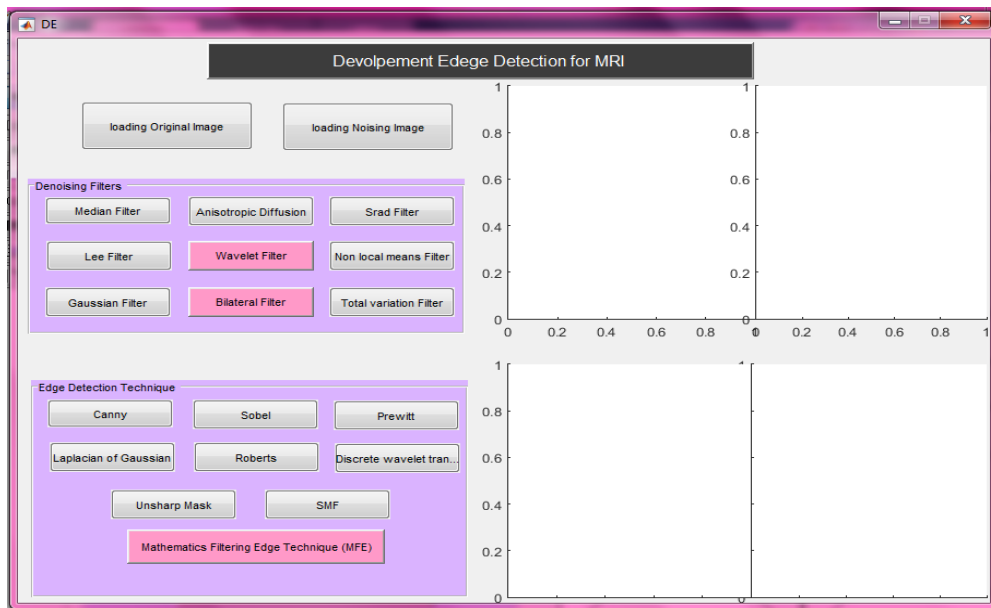
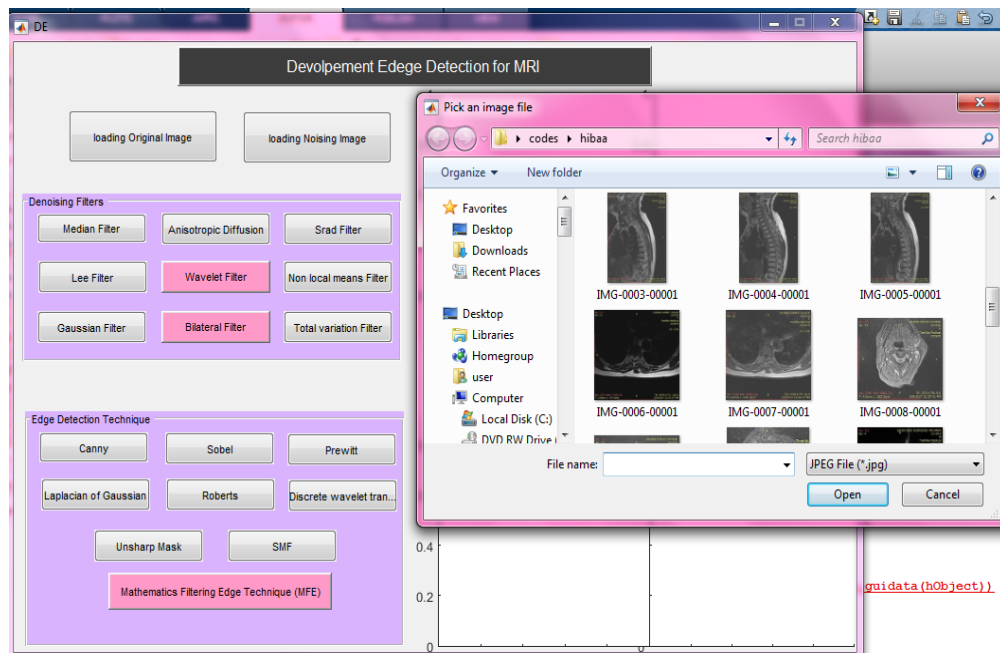


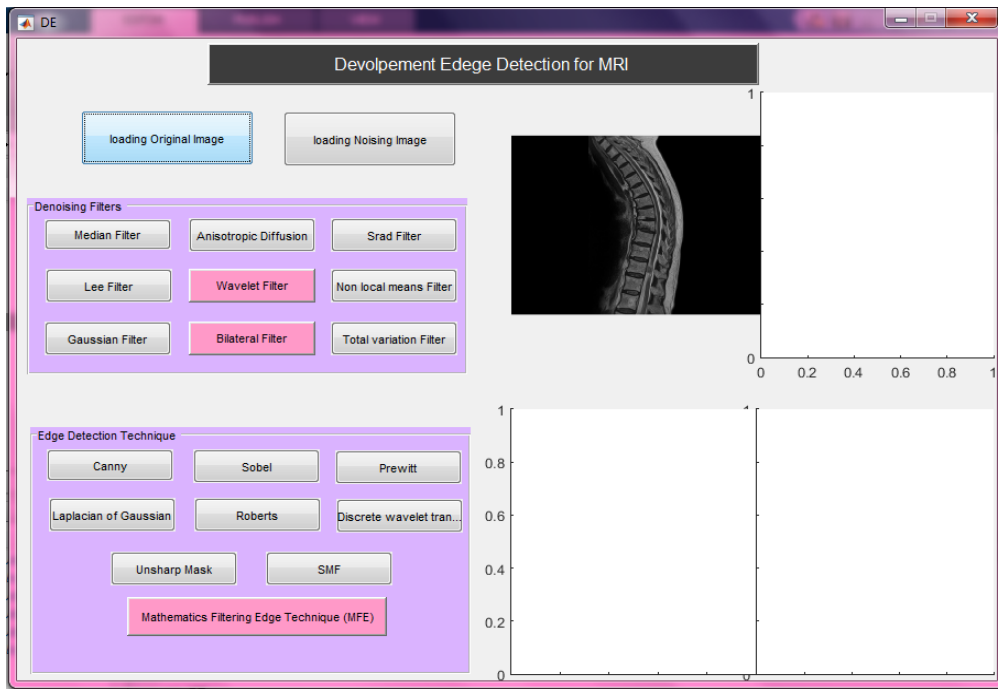
Figure 5-18 : Graphical User Interface (GUI)

Parameter in GUI

- Load image



a) loading image



b) Image select

Figure 5-19: use GUI to load image

Noise and filtering

- Gaussian noise

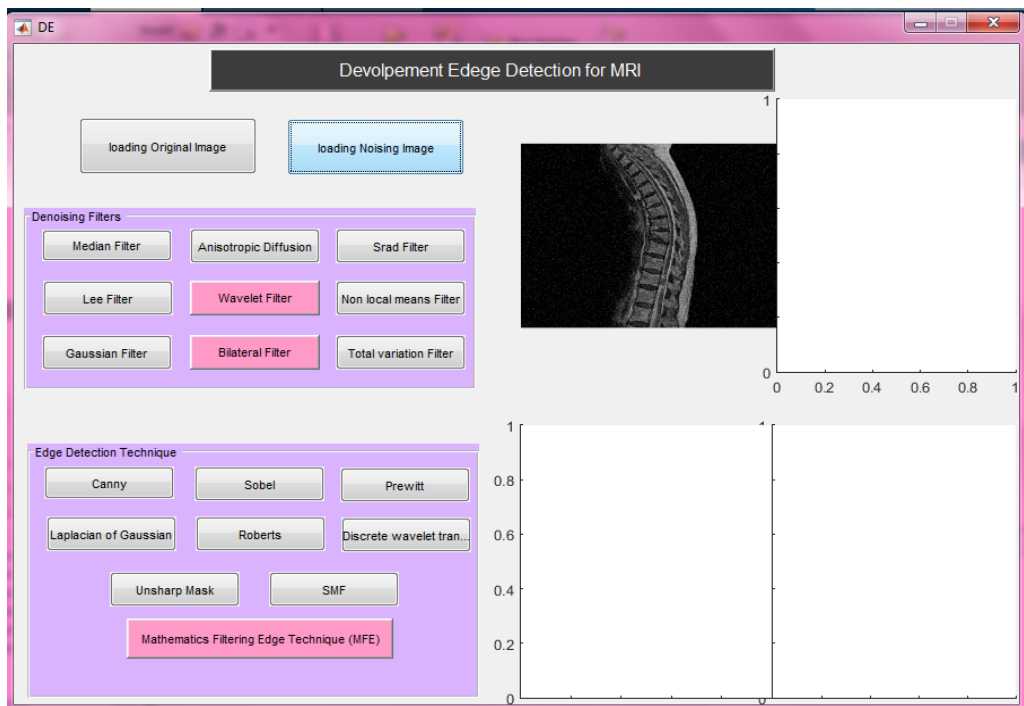
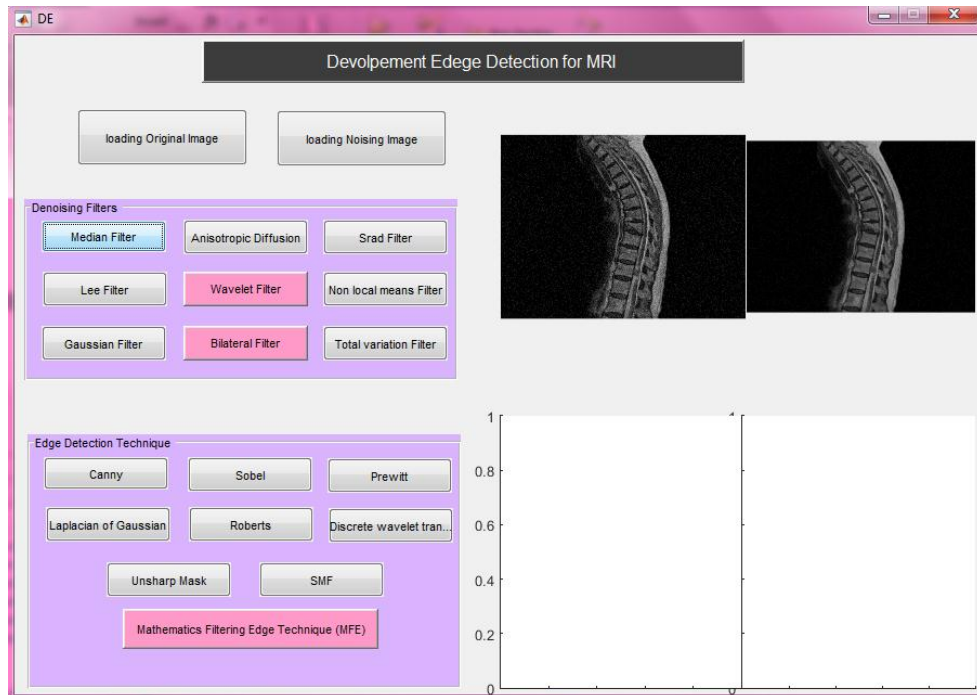


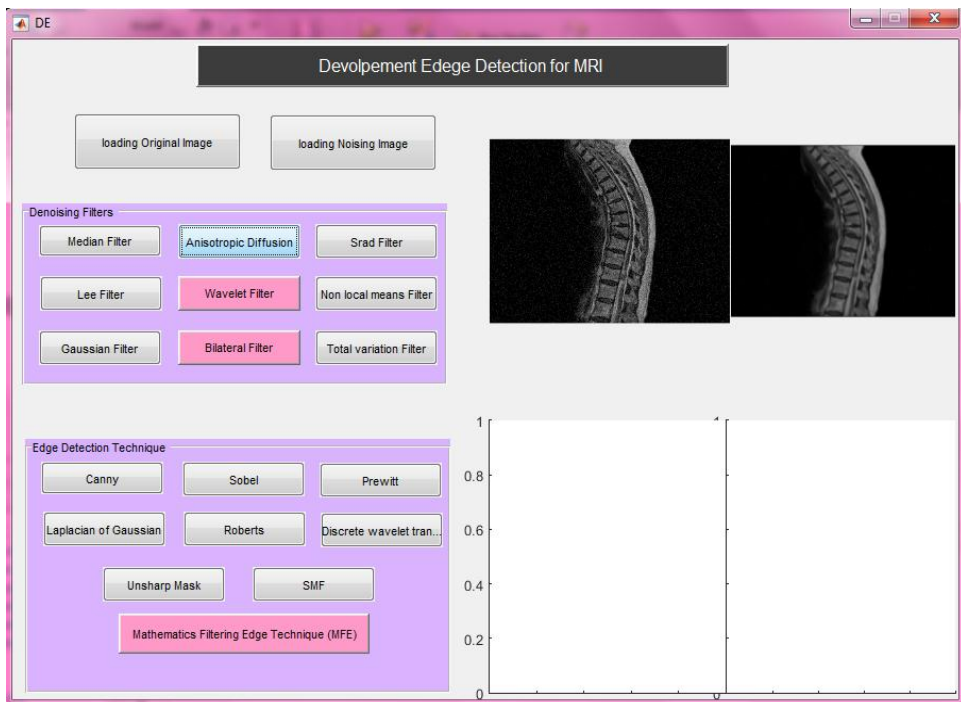
Figure 5-20 : Addition of Gaussian noise to image

- Median filter



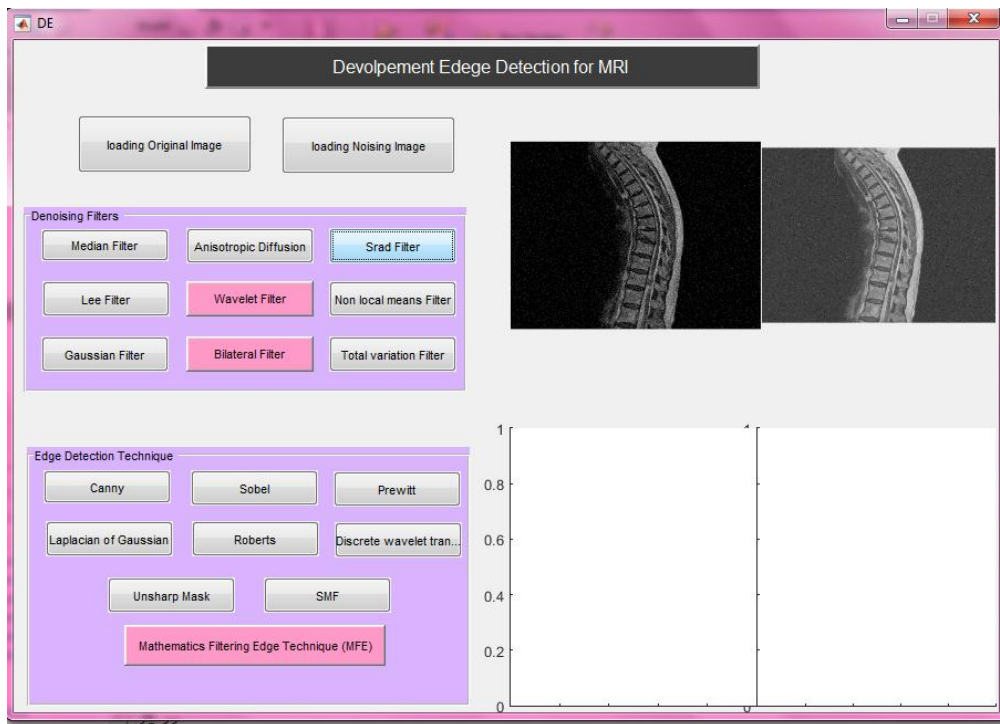
a) Gaussian noise filtered with Median filter

- Anisotropic diffusion filter



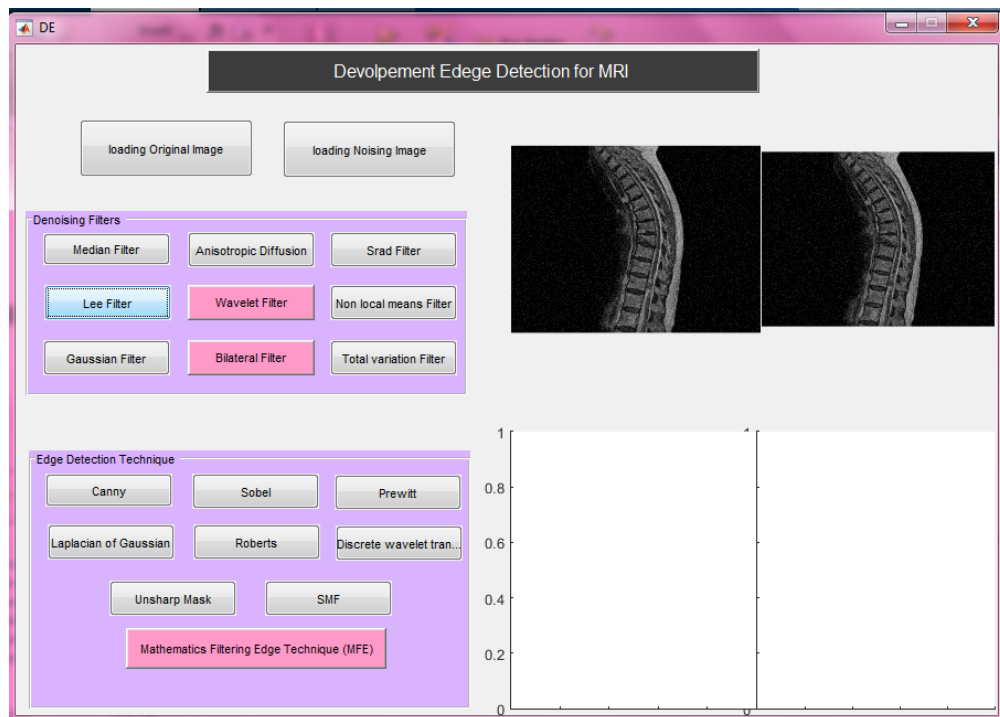
b) Gaussian noise filtered with anisotropic diffusion filter

- SRAD filter



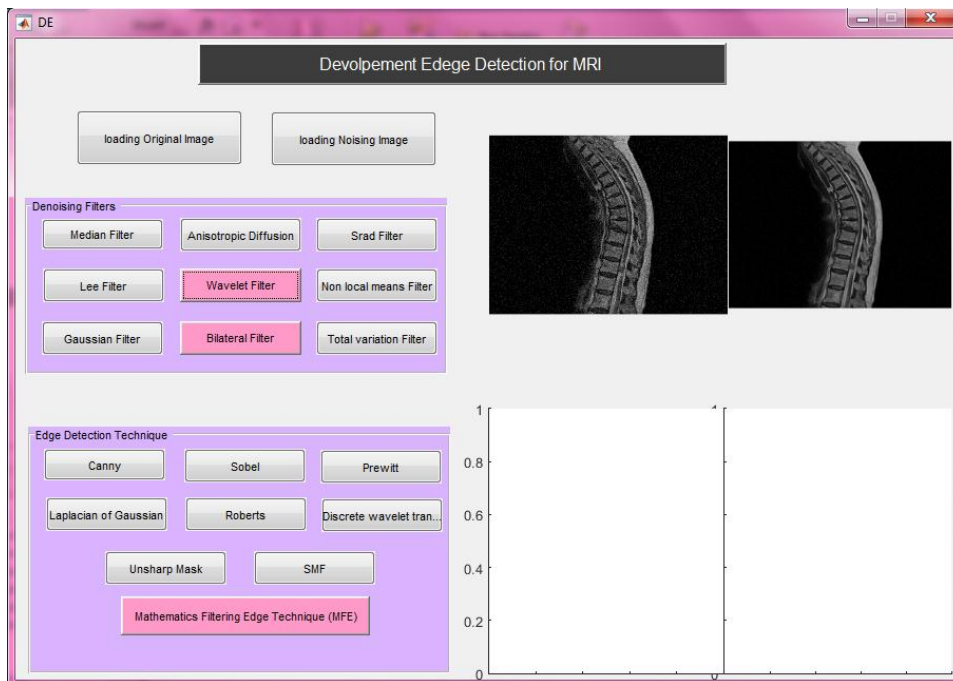
c) Gaussian noise filtered with SARD filter

- Lee filter



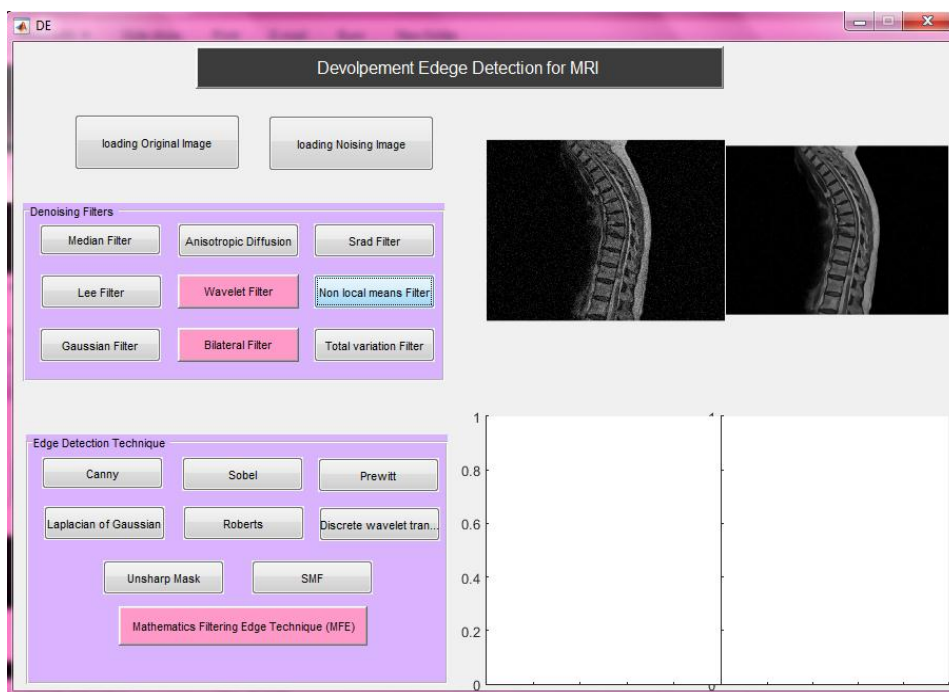
d) Gaussian noise filtered with Lee filter

- Wavelet filter



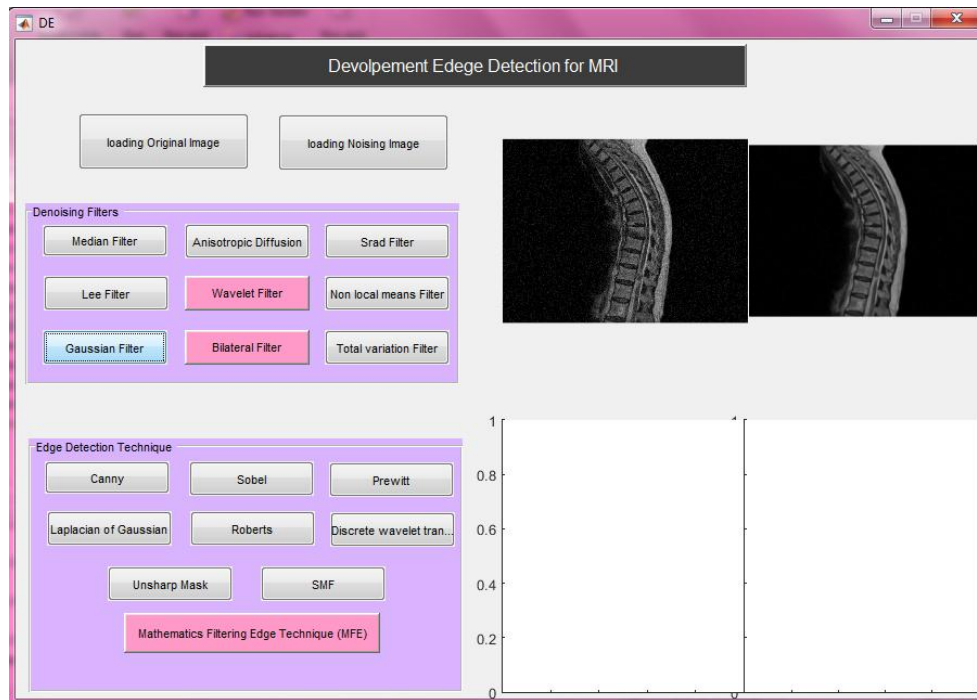
e) Gaussian noise filtered with wavelet filter

- Nonlocal mean filter



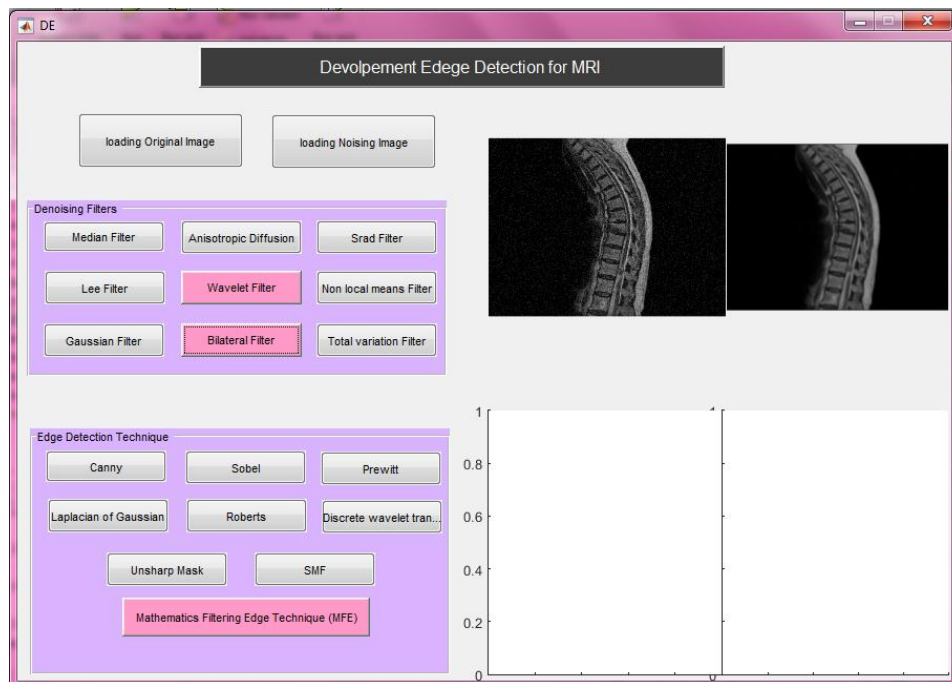
f) Gaussian noise filtered with nonlocal means filter

- Gaussian filter



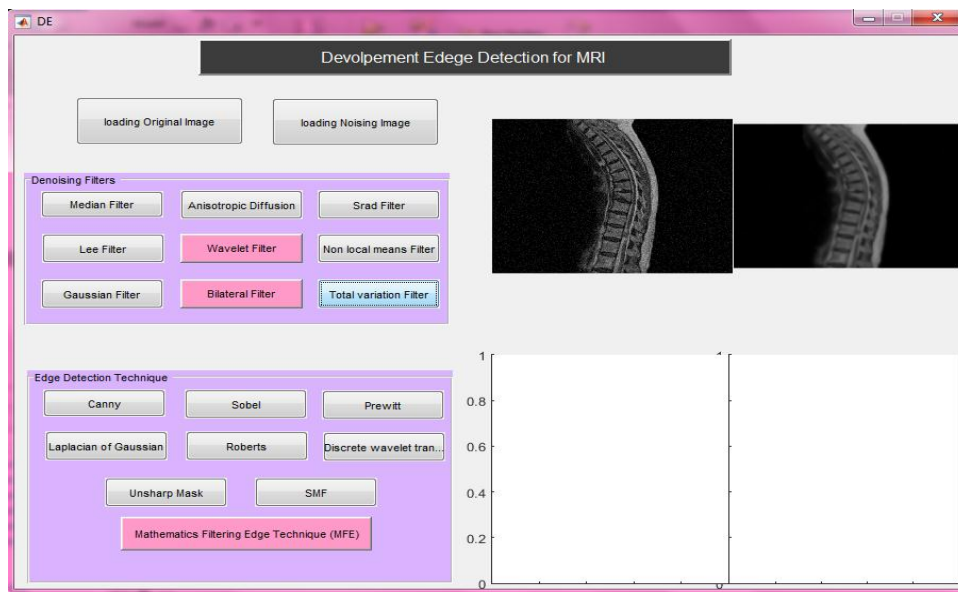
g) Gaussian noise filtered with gaussian filter

- Bilateral filter



h) Gaussian noise filtered with bilateral filter

- Total Variation filter



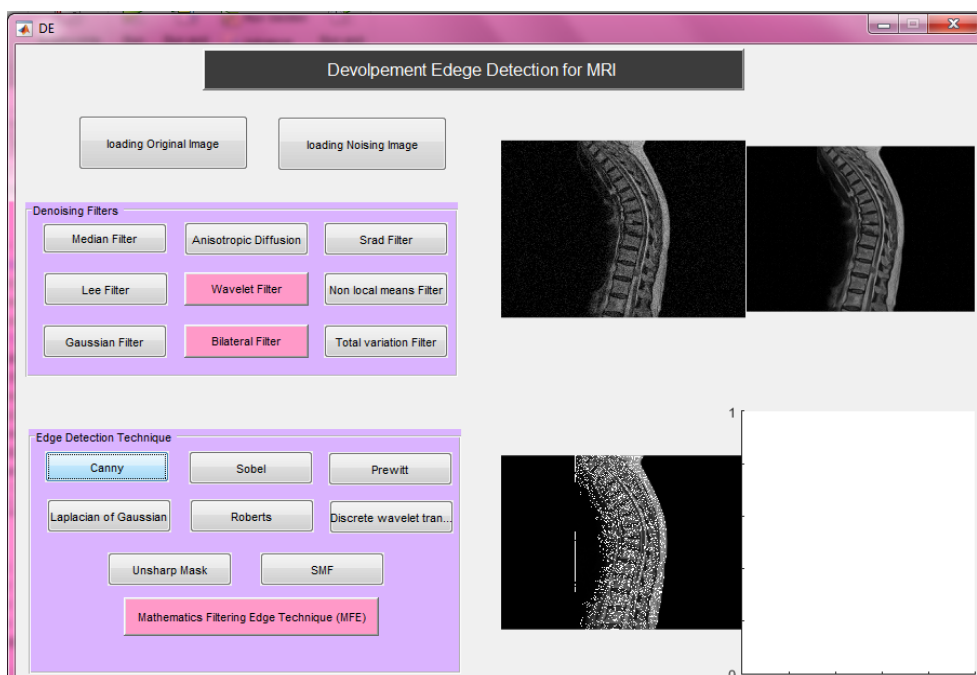
i) Gaussian noise filtered with total variation filter

Figure 5-21: From a to i Use GUI to show the results of applying the different types of filter to Gaussian noise image.

Figure (5-21) From a to i show the results of applying the noise (Gaussian) and filtering the images (Median, Anisotropic diffusion, SRAD, Lee, Wavelet, Gaussian, Bilateral, Total variation and NLM filters).

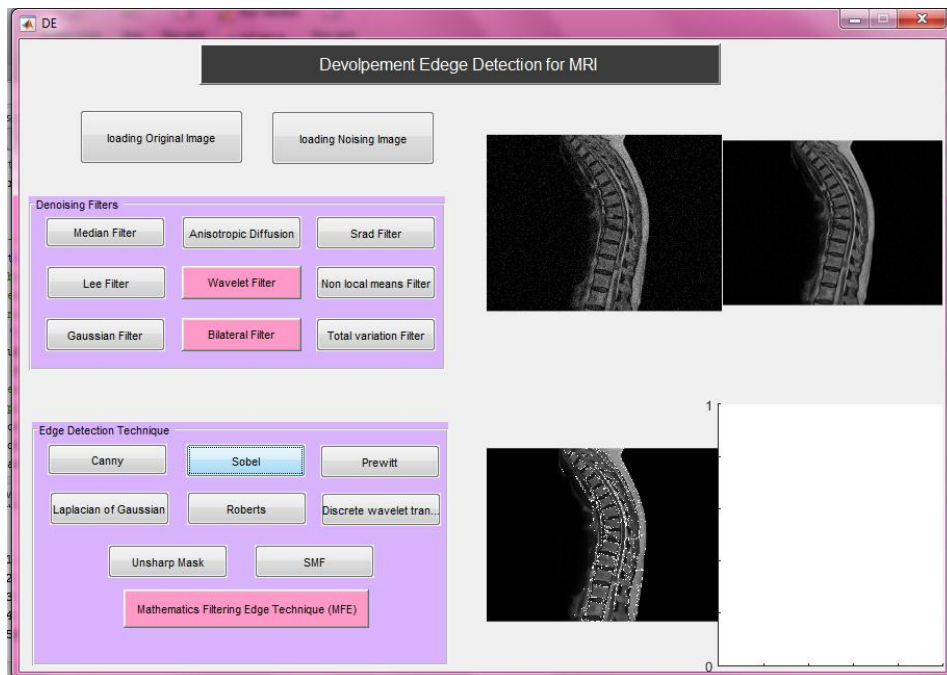
Edge detection technique

- Canny Operator



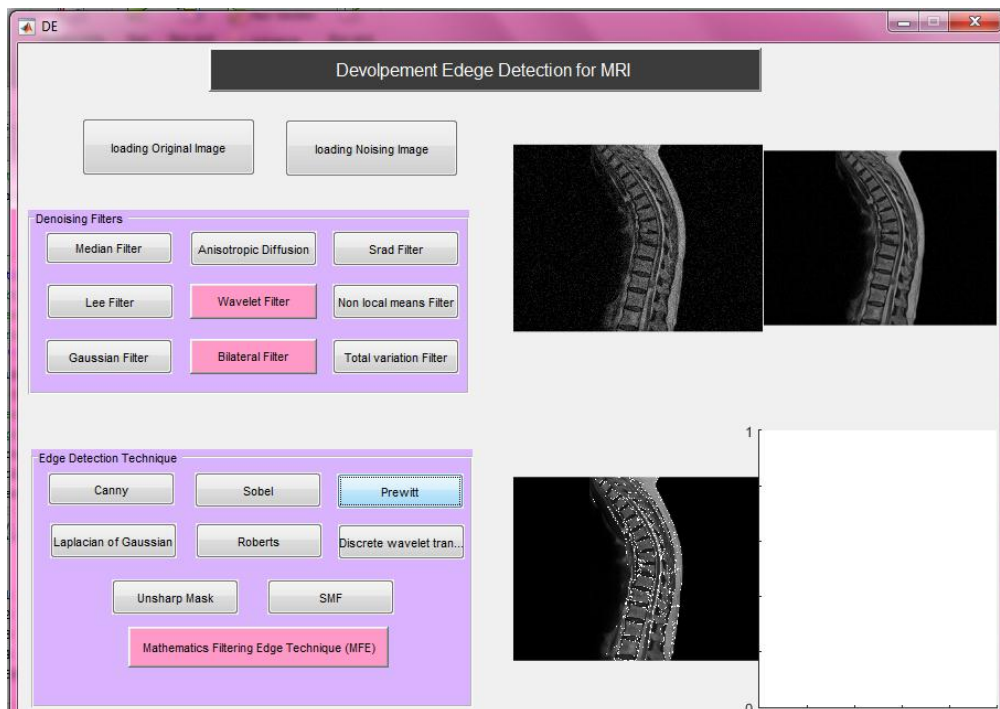
a) Canny operator applied to image

- Sobel operator



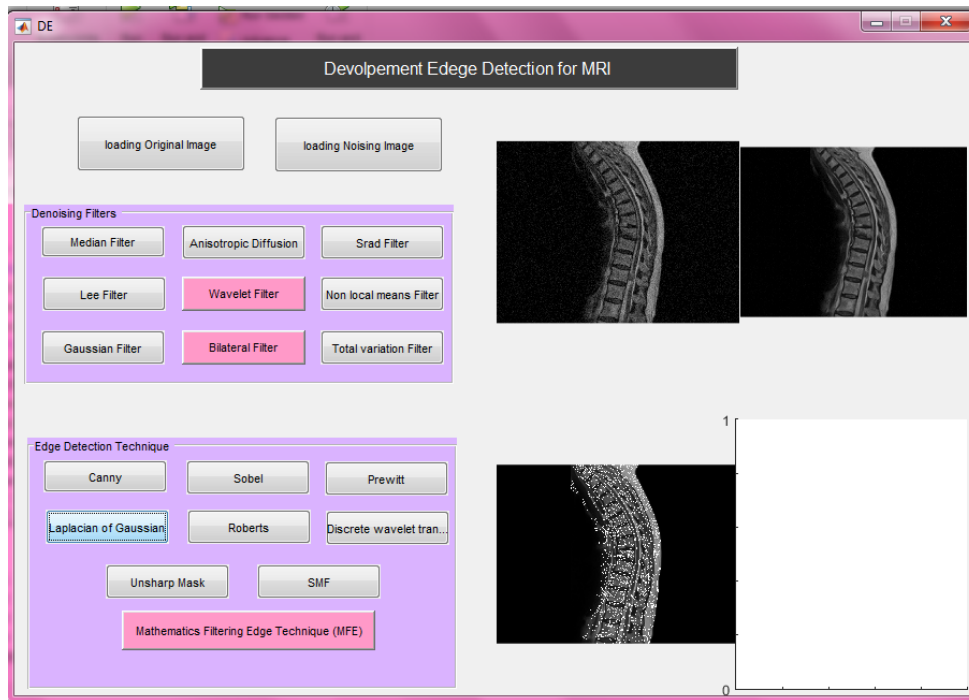
b) Sobel operator applied to image

- Prewitt Operator



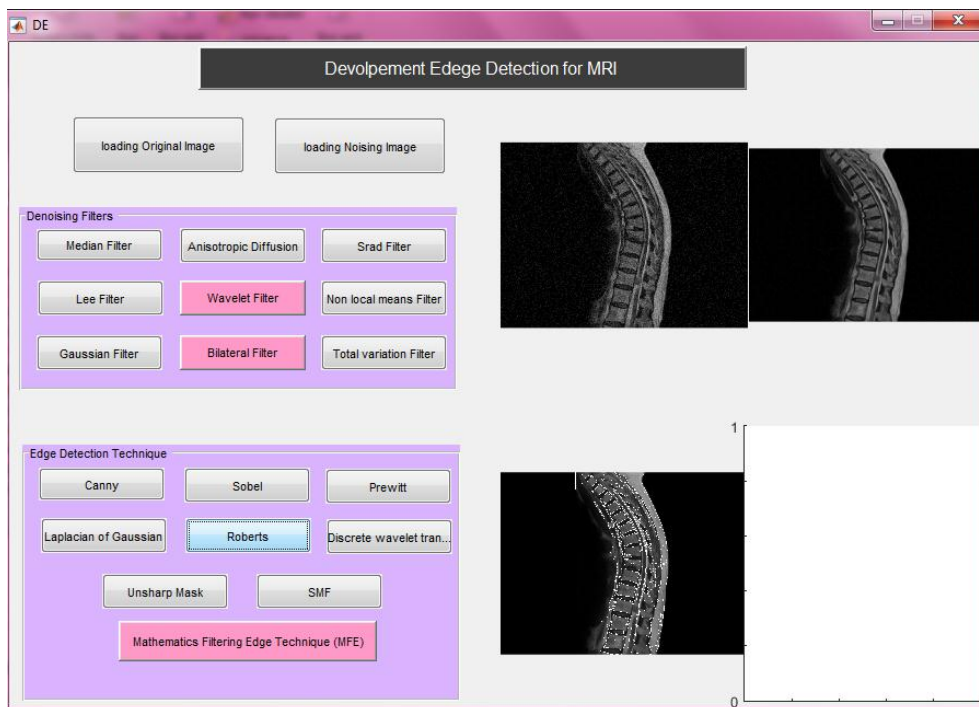
c) Prewitt operator applied to image

- LoG Operator



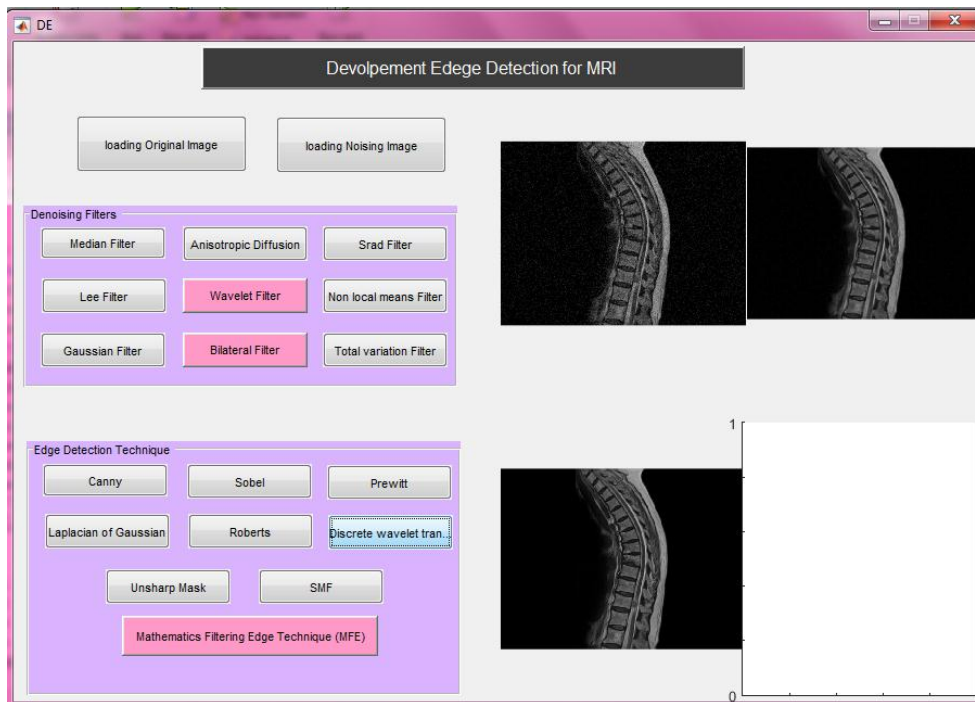
d) LoG operator applied to image

- Roberts Operator



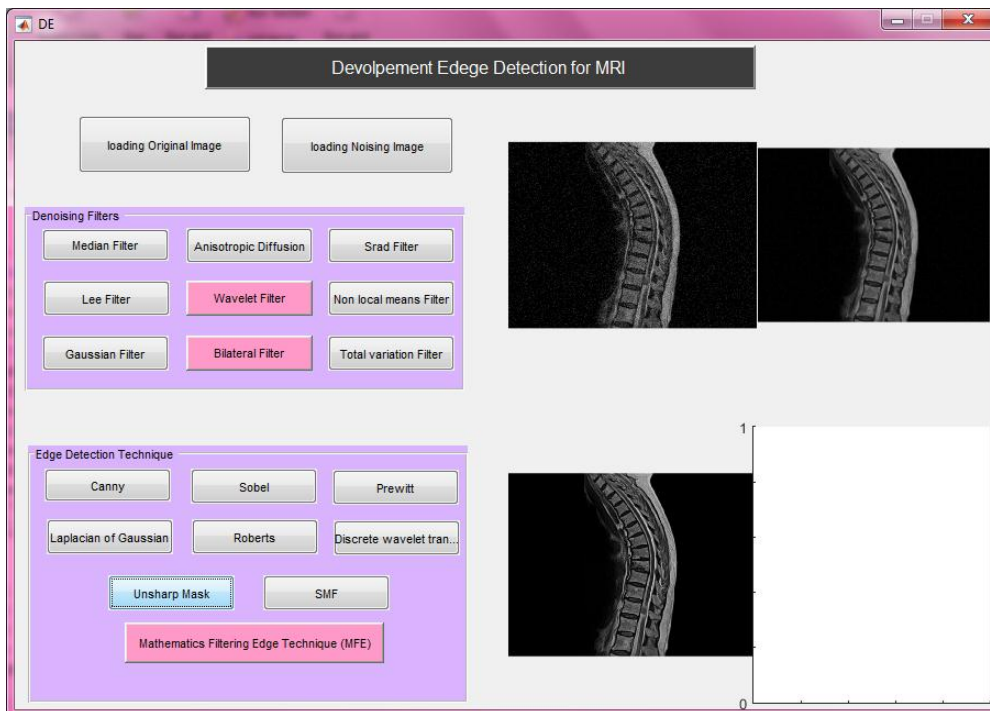
e) Roberts operator applied to image

- Wavelet (haar) technique



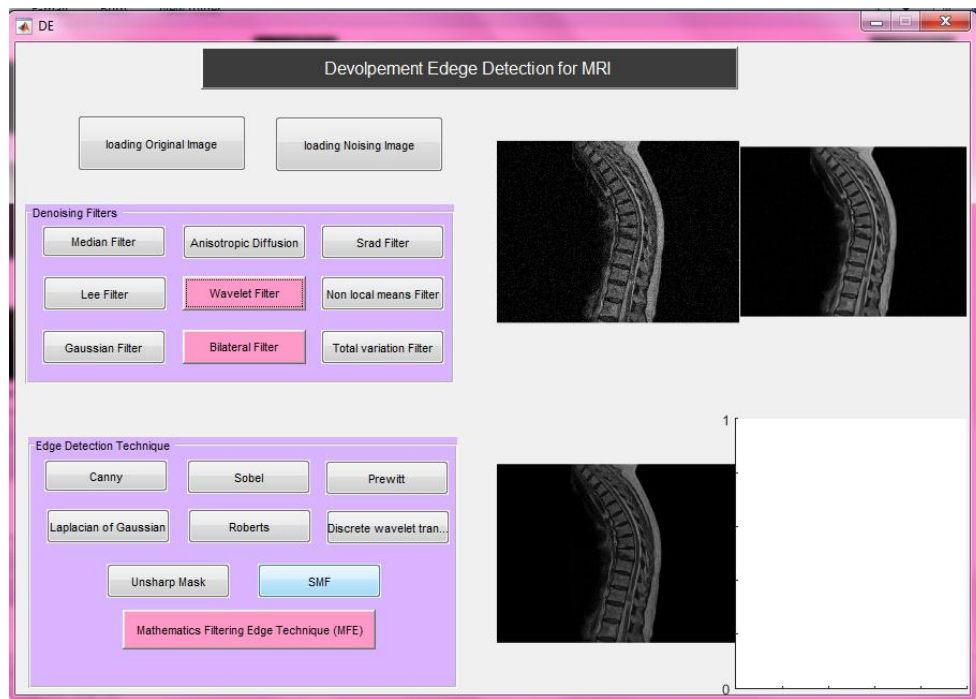
f) wavelet (haar) edge detection technique applied to image

- Unsharp mask technique



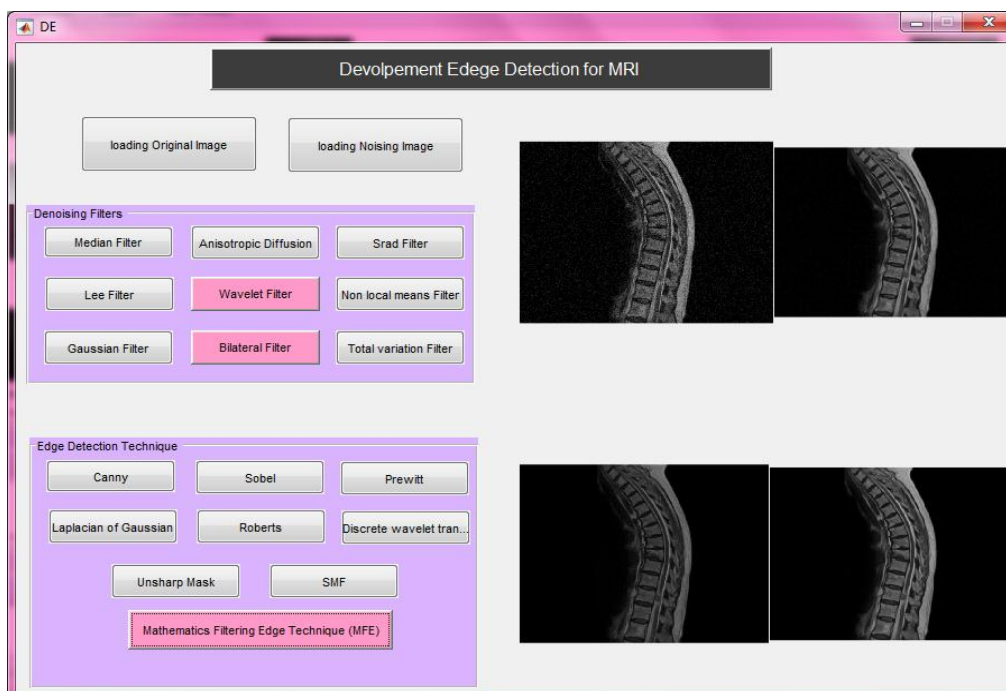
g) Unsharp mask edge detection technique applied to image

SMF



h) Structural mathematic filtering edge detection technique applied to image

MFE



i) Mathematics Edge Technique Filtering applied to image

Figure 5-22: From a to i Use GUI to show the results of applying the edge detection techniques .

5.2 Discussion

The results mentioned above, noise and filtering, edge detection for standard image, edge detection for real image and GUI, were briefly discussed. The performance of the spatial filters was shown in table 5-1 and figure 5-2. These spatial filters have been evaluated by the results of MSE, SNR, PSNR and elapsed time. When the value of the MSE is low, both the SNR and PSNR are high and elapsed time is high, the filter in this case is considered to be the best filter to be used. According to the results obtained in the table below the previous characteristics were presented in both the wavelet and bilateral filter.

The performance of the edge detection techniques was shown in table 5-2 and figure 5-16. These techniques have been judged by the result of MSE, SNR, PSNR and elapsed time. As mentioned earlier, when the value of the MSE is low, both the SNR and PSNR are high and elapsed time is high, the technique in this case is considered to be the best technique to be used. When comparing between the nine techniques the (sobel, canny, LoG, prewitt and roberts operators and the wavelet transform, Unsharp mask, SMF and METF) it was found that the sobel, robert, prewitt and LoG operators sensitivity to noise is inaccurate, moreover the LoG couldn't find the orientation of edge because of using the Laplacian filter and canny operator complex computations and MSE is high, and the Unsharp mask also had a high MSE and low SNR and PSNR. wavelet transform had the low MSE but also low SNR and PSNR, and the SMF has a slightly high MSE and low SNR and PSNR and it takes a very long time to execute. while the METF had a best MSE and better SNR and PSNR from the other techniques as shown in the table above.

The final part was the GUI which was done to simplify the application of the techniques and functions on the images used in this thesis.

Chapter Six

6 Conclusion and Recommendation

6.1 Conclusion

In this thesis nine edge detection techniques were applied to a MRI image. From the nine techniques discussed the METF technique was found to be the best, compared to the Canny, Roberts, Prewitte, Soble and LoG operators, Discrete Wavelet Transform (haar), Unsharp mask and SMF edge detection.

In the METF technique, a sharpen filter was applied to the original image, then subtracted the sharpened image from the original image. This subtracted resulted in an edge, which was added to the original image. Afterward it was applied to the Wavelet Thresholding filter to the sharpened image. Then the bilateral filter was applied to the image obtained from subtracting the original image from the sharpened image. After the images obtained from adding edge to original image, and the Wavelet Thresholding filter was applied and bilateral filter was filter and finally were added together. The results of these techniques were evaluated by comparing the values of the MSE, SNR, PSNR and elapsed time. The final step was creating a GUI to simplify the application of the techniques mentioned above.

6.2 Recommendation

The following recommendations are suggested:

1. Apply this technique on various images like Computed Tomography (CT) and Ultrasound (US) images.
2. Use other filters to develop edge detection techniques.
3. Use different mathematical equations.
4. Development previous techniques to increase their efficiency.

References:

- [1] M.I. Rajab, M.S. Woolfson, and S.P. Morgan, "Application of region-based segmentation and neural network edge detection to skin lesions," *Computerized Medical Imaging and Graphics*, vol. 28, pp. 61–68, 2004.
- [2] H. Tang, E.X. Wu, Q.Y. Ma, D.Gallagher, G.M. Perera, and T. Zhuang, "MRI brain image segmentation by multi-resolution edge detection and region selection," *Computerized Medical Imaging and Graphics*, vol 24, pp. 349–357, 2000.
- [3] ShahidEqbal Dr. M. A. Ansari Assoc," *Medical Image Feature Extraction for Computer Aided Diagnosis of Lung Cancer*," *International Journal of Advanced Research in Computer Science and Software Engineering Research*, Volume 5, Issue 6, June 2015.
- [4] AnamikaAhirwar , and R.S. Jadon, "Evaluation and comparison of features of brain MRI," *International Journal of Computer Engineering*, Volume 3, Number 1, pp. 11–22 , January-June 2011.
- [5] www.cse.usf.edu/.../MachineVisionBook/MachineVision.../MachineV..
- [6] P. Mohankumar, Leong Wai Yie, "Edge Detection of The Scoliotic Vertebrae using X-ray," *Journal of Engineering Science and Technology*, EURECA 2015 Special Issue February (2016) 166 – 175.
- [7] Claudia I. GonzalezPatriciaMelinJuan R. CastroOliviaMendozaOscar Castillo, Gonzalez, C.I., Melin, P., Castro, J.R. et al., " An improved sobel edge detection method based on generalized type-2 fuzzy logic," *SoftComput* (2016) 20: 773.
- [8] Bindu Bansal, Jasbir Singh Saini, Vipin Bansal, and Gurjit Kaur , "Comparion of Various Edge Detection Techniques," *Journal of Information and Operations Management* ISSN: 0976–7754 & E-ISSN: 0976–7762 , Volume 3, Issue 1, 2012, pp-103-106.
- [9] Raman Maini& Dr. HimanshuAggarwal, "Study and Comparison of Various Image Edge Detection Techniques," *Punjabi University, Patiala-147002(Punjab), India*, *International Journal of Image Processing (IJIP)*, Volume (3) : Issue (1)
- [10] JamilaHarbi, Batooldaraam, Waseem M. Ali, "Edge Detection in Ultrasound Images Based on Modified Unsharp and Wavelet transform Filters," *University of Technology, Iraqi*, *International Letters of Chemistry, Physics and Astronomy* Vol. 52 (2015) pp 90-99.
- [11] John Wiley & Sons, "Medical Imaging: Principles, Detectors, and Electronics", edited by Krzysztof Iniewski Copyright ,2009 .

- [12] Milindkumar V. Sarode, Dr. Prashant R. Deshmukh, " Performance Evaluation of Noise Reduction Algorithm in Magnetic Resonance Images", *IJCSI International Journal of Computer Science Issues*, Vol. 8, Issue 2, March 2011.
- [13] Tzu-Heng Henry Lee, "Edge Detection Analysis", National Taiwan University, Taipei, Taiwan, ROC, E-mail: r96942133@ntu.edu.tw.
- [14] Iza Sazanita Isa¹, Siti Noraini Sulaiman¹, Muzaimi Mustapha², Sailudin Darus¹, " Evaluating Denoising Performances of Fundamental Filters for T2-Weighted MRI Images", *19th International Conference on Knowledge Based and Intelligent Information and Engineering Systems*, *Procedia Computer Science* 60 (2015) 760 – 768.
- [15] V N Prudhvi Raj and Dr T Venkateswarlu, " Denoising of Magnetic Resonance and X-ray Images using Variance Stabilization and Patch Based Algorithms ", *The International Journal of Multimedia & Its Applications (IJMA)* Vol.4, No.6, December 2012.
- [16] Milindkumar V. Sarode¹, Dr. Prashant R. Deshmukh², " Performance Evaluation of Noise Reduction Algorithm in Magnetic Resonance Images",. *IJCSI International Journal of Computer Science Issues*, Vol. 8, Issue 2, March 2011 ISSN (Online): 1694-0814 ,www.IJCSI.org
- [17] Hodder Arnold , "Introduction to medical imaging", *Imaging for Students* © 2012 David A Lisle
- [18] R.C.Gonzalez and R.E.Woods, *Digital image Processing*, Addison-Wesley Publishing Company, 1992, second edition.
- [19] Gregory A.Baxes, *Digital Image Processing*, Jone Wiley & Sons, Inc. 1994.
- [20] Tarandeep Chakra , *Genetic Dua*, Trite Malhotra (*Comparative Analysis of Methods to De-noise CT Scan Images*) Vol. 2, Issue 7, July 2013
- [21] nuha , *hybrid technique for noise removal from CT image*
- [22] Ahmed s. Mashaly, Ezz Eldin F. AbdElkawy and Tarek A. Mahmoud, "Speckle Noise Reduction in SAR image Using Adaptive Morphological Filter", *10th International Conference on Intelligent Systems Design and Application*, 2010.
- [23] https://en.wikipedia.org/wiki/Non-local_means#Definition
- [24] Yang, Q., Tan, K.H., Ahuja, N.: *Real-time o(1) bilateral filtering*. CVPR (2009)
- [25] Adams, A., Gelfand, N., Dolson, J., Levoy, M.: *Gaussian kd-trees for fast high dimensional*
- [26] Liu, C., Freeman, W.T., Szeliski, R., Kang, S.B.: *Noise estimation from a single image*. CVPR (2006)

- [27] Fattal, R., Agrawala, M., Rusinkiewicz, S.: *Multiscale shape and detail enhancement from multi-light image collections. SIGGRAPH (2007)*
- [28] Kopf, J., Cohen, M., Lischinski, D., Uyttendaele, M.: *Joint bilateral up sampling. SIGGRAPH (2007)*
- [29] Yuan, L., Sun, J., Quan, L., Shum, H.Y.: *Progressive inter-scale and intra-scale non-blind image De-convolution. SIGGRAPH (2008)*
- [30] Tomasi, C., Manduchi, R.: *Bilateral filtering for gray and color images. ICCV (1998)*
- [31] Bae, S., Paris, S., Durand, F.: *Two-scale tone management for photographic look. SIGGRAPH (2006)*
- [32] Paris, S., Durand, F.: *A fast approximation of the bilateral filter using a signal processing approach. ECCV (2006)*
- [33] Porikli, F.: *Constant time $o(1)$ bilateral filtering. CVPR (2008)*
- [34] Petschnigg, G., Agrawala, M., Hoppe, H., Szeliski, R., Cohen, M., Toyama, K.: *Digital photography with flash and no-flash image pairs. SIGGRAPH (2004)*
- [35] Durand, F., Dorsey, J.: *Fast bilateral filtering for the display of high-dynamic-range images. SIGGRAPH (2002)*
- [36] Zeinab A. Mustafa, Yasser M. Kadah, *Multi Resolution Bilateral Filter for MR Image Denoising*
- [37] <https://en.wikipedia.org/wiki/Wavelet>
- [38] https://en.wikipedia.org/wiki/Anisotropic_diffusion
- [39] https://en.wikipedia.org/wiki/Total_variation_denoising
- [40] https://en.wikipedia.org/wiki/Median_filter#
- [41] Scott T. Acton, Janelle A. Molloy and Yongjian Yu, "Three-Dimensional Speckle Reduction Anisotropic Diffusion", *IEEE Conference Record of the 37th Asilomar Conference on Signals, Systems and Computer*, vol2, pp: 1987- 1991, 2003.
- [42] J.Canny, "A Computational Approach to Edge Detection", *IEEE PAMI*, VOL.8, NO.6, November 1986.
- [43] *Computed Tomography (CT) - Head, Radiology Information, Copyright © Feb-12-2014.*

- [44] V.S. Nalwa and T.S. Binford, *On Detecting Edge*, IEEE Trans. PAMI. VOL. 8, NO. 6, pp699-714, November 1986.
- [45] Raman Maini & Dr. Himanshu Aggarwal, "Study and Comparison of Various Image Edge Detection Techniques", *International Journal of Image Processing (IJIP)*, Volume (3) : Issue (1), Patiala-147002(Punjab), India
- [46] Muthukrishnan.R and M.Radha, "EDGE DETECTION TECHNIQUES FOR IMAGE SEGMENTATION", *International Journal of Computer Science & Information Technology (IJCSIT)* Vol 3, No 6, Dec 2011.
- [47] P.Deepa and M.Suganthi , "Performance Evaluation of Various Denoising Filters for Medical Image", (IJCSIT) *International Journal of Computer Science and Information Technologies*, Vol. 5 (3) , 2014, 4205-4209
- [48] Zhen Zhang, Siliang Ma, Hui Liu , Yuexin Gong, "An edge detection approach based on directional wavelet transform", *Computers and Mathematics with Applications* 57 (2009) 1265_1271, journal homepage: www.elsevier.com/locate/camwa
- [49] Yahia S. Alhalabi, Hesham Jondi Abd, "New Wavelet-Based Techniques for Edge Detection ", *Computer Science Department, Princess Sumaya University for Technology Amman , AL-Jubaiha, Jordan, Journal of Theoretical and Applied Information Technology*, © 2005 - 2010 JATIT & LLS. All rights reserved.
- [50] Ahmed Nageib, "Development of edge detection technique using structure, mathematics filtering and graphical user interface (GUI) for CT images", *University of Science and Technology, College of Postgraduate Studies and Academic Advancement, Faculty of Engineering, Department of Biomedical Engineering Khartoum, Sudan, May (2016).*